FINAL TECHNICAL REPORT

IDENTIFICATION AND MODELING OF SOIL-STRUCTURE-INTERACTION FOR AN ANSS INSTRUMENTED BUILDING: COLLABORATIVE RESEARCH WITH THE UNIVERSITY OF ALASKA ANCHORAGE AND THE UNIVERSITY OF VIRGINIA

Principal Investigators:

He (Helen) Liu
School of Engineering
University of Alaska Anchorage
3211 Providence Drive, Anchorage, AK 99508
Phone: (907) 786-1971, Fax: (907) 786-1079
Email: afhl@uaa.alaska.edu

Yibin Zheng
G E Medical Systems
N25w23255 Paul Rd
Pewaukee, WI 53072
Phone: (262) 524-5126, Fax (262) 869-2790
Email: yibin.zheng@gmail.com

U.S. Geological Survey
National Earthquake Hazard Reduction Program
Award No. 07HQGR0073 and 07HQGR0065

March 10, 2008

Research supported by the U.S. Geological Survey (USGS), Department of the Interior, under USGS award numbers 07HQGR0073 and 07HQGR0065. The views and conclusions contained in this document are those of the authors and should not be interpreted as necessarily representing the official policies, either expressed or implied, of the U.S. Government.

Abstract

The goal of this proposal is to develop a system identification tool to estimate structure and site dynamic properties for the purpose of creating the baseline soil-structure-interaction (SSI) model for Robert B. Atwood Building (AB), using state-of-the-art system identification and modeling techniques for the building structure and soil site.

Field experience has shown that SSI can mitigate the most violent seismic accelerations experienced during severe earthquakes but can also create unpredictable impacts to large mat foundation systems. Current understanding of SSI is limited, and methods for including SSI effects in building design and analysis are limited to a few simple procedures identified in building codes (NEHRP 2003 and ASCE 7-02).

One of the major contributing factors to the lack of understanding of SSI effects is the limited availability of strong motion data from building instrumentation directly accompanied by seismic motion data of the adjacent soil. The AB and the surrounding site have been electronically monitored to record motion during seismic events. While the NSF EPSCoR program sponsored an adjacent downhole array construction, the building and the downhole array were fully instrumented through the Advanced National Seismic System (ANSS) of the U.S Geological Survey. The building is instrumented to capture horizontal motion in two directions on ten floors. Vertical and rocking motion is captured by three sensors. This instrumentation presents an enormous opportunity for investigation and research of SSI effects.

Beyond building and site instrumentation, one of the most critical requirements for SSI investigation is the development of a computerized tool to estimate the existing structure and soil dynamic properties for the purpose of generating accurate and reliable analysis models for the soil-structure system. The objective of the project is to develop a system identification tool to identify the structure and site dynamic properties. To achieve this objective, we apply novel approaches to: (a) develop a simplified two-dimensional shear-bending type structural model suitable for the AB; (b) generate a systematic procedure to complete the structural response data from the incomplete recorded data set; (c) develop the system identification tool based on the extended Kalman filter (EKF) for single-input multi-outputs (ground-input story-response-outputs) conditions for the purpose of estimating the inter-story stiffness for a low-rise multi-story structure; (d) develop the system identification tool for a simplified shear-bending chain type structure, like the AB, to estimate the inter-story stiffness from the recorded seismic response data; (e) develop the system identification tool based on the extended Kalman filter (EKF) for single-input multi-outputs (bedrock-input downhole-array-outputs) conditions to identify the stiffness for layered soil sited. The outcome from this project will provide a tool to create simplified structural and site models the AB and similar building in future SSI analysis.

Table of Contents

Abstract i
Table of Contents ii

1. Introduction 1

2. The Building and Site Description 2
2.1 The Building and Site 2
2.2 The Building and Downhole Instrumentation 3

3. System Identification Method-Extended Kalman Filter 4
3.1 The extended Kalman filter 4
3.2 The First-Order Polynomial Approximations 6

4. Modeling and Identification Procedure 7

5. Conclusion 8

Appendix A 10
Simplified Two-Dimensional Shear-Bending Structural Model 10

Appendix B 15
Method of Displacement Interpolation at Intermediate Non-Instrumented Levels 15

Appendix C 18
System Identification of the Inter-Story Stiffness for Shear Type Low-Rise Multi-Story Structures Using the Extended Kalman Filer 18

Appendix D 19
System Identification of the Inter-story Stiffness for High-Rise Building Structures Using the Extended Kalman Filter and Recorded Seismic Data 19
D.1 Introduction 19

D.2 Identification Procedure 19

D.3 Decoupling Algorithm for the Mass-Spring-Damping System 20

D.4 Extended Kalman filter for the Decoupled SDOF system 22

D.5 Simulation Example 23

D.6 Conclusion 27

Appendix E 28

System Identification of Model Parameters for Layered Soils Using the Extended Kalman with the Recorded Seismic Data from the Downhole Array of Atwood Building 28

E1. Introduction 28

E3. Identification of the parameters of MDOF shear model using recorded seismic data 30

E4. Identification example 33

E5. Verification of identified results 37

E6. Conclusions 39

References 40

Acknowledgements 42

Bibliography 43

1. Introduction

Assessments of seismic loading for structures must appropriately characterize interaction of soil with the structure (SSI). The extent to which the SSI alters the system response varies from negligible to profound and is mostly dependent on the stiffness of the soil relative to the structure. Many critical questions concerning the dynamic response of SSI systems and failure characteristics in an in-situ environment remain unanswered. Simplified substructure-based SSI provisions are included in the National Earthquake Hazard Reduction Program codes (NEHRP 2003; Holmes 2000; ASCE 7-02 2003), but these provisions need to be calibrated against field performance data. Quantitative understanding of the effects of ground motion on SSI systems can be achieved only by the instrumental measurements of the dynamic response of the SSI systems during an earthquake. Many important buildings and structures throughout the United States have been instrumented for quantitative measurements of the response and to provide detailed understanding of the SSI effect (Celebi, 2000; 2005; 2006).

Anchorage and its surrounding areas belong to one of the most seismically active hazard zones in the world. The 0.2 second spectral response acceleration (5% of critical damping) is around 1.65g (maximum considered earthquake ground motion) with 2% probability of exceedence in 50 years (NEHRP 2003). The megathrust zone lies at a depth of about 35 km beneath Anchorage; the Great Alaska Earthquake (M_W=9.2) of 1964 was located along this zone. The region suffered widespread damage during this great earthquake due to the extensive ground shaking. Various types of soil-related failures occurred including soil liquefaction, subsidence, consolidation, cracks, and sand spouts. The typical soil conditions and frequent earthquakes make Anchorage an idea place for SSI investigation.

Instrumental measurements should include ground surface, subsurface and structure. In Anchorage and the surrounding area, the surface instrumentation network has almost completed with more than 40 accelerometer stations on the surface and one station at the hard rock. Several instrumented structures include a long bridge, several steel moment frame buildings and one multi-story reinforced concrete building. Among these, a 20-story office building, the Robert B. Atwood Building (AB) was fully instrumented with 36 accelerometer channels at 10 level in the building plus 21 channels in the downhole array near the AB. The completion of the downhole array and AB instrumentation makes the system unique for SSI investigation in the natural seismic laboratory of Alaska. The proposed project will be a part of efforts of SSI study focusing on modeling technique of SSI systems, typically for modeling of the AB downhole array and the building system.

There are great analytical challenges in the development of appropriate nonlinear SSI modeling techniques. This project is focused on meeting these challenges utilizing the well-instrumented AB**.** In this proposal, a new identification tool using the extended Kalman filter (EKF) will be developed to identify the structural and site dynamic properties with the recorded seismic data from the instrumented building and downhole array.

The identification approach will play a significant role in the calibration of the Finite Element (FE) models for the structure of the AB, in the observation of its site response variations,

and in the identification of possible damage of the building or unsatisfactory performance of soil in future damaging earthquake events.

2. The Building and Site Description

2.1 The Building and Site

The AB is a steel framed building; the lateral resisting system consists of steel moment resisting frames and interior steel shear walls. The foundation system consists of a concrete mat. The AB in the downtown area of Anchorage is owned by the State of Alaska and was designed in 1981 based on UBC 1979 Edition. The structure is 20 stories (including the mechanical & electrical floors, plus a basement that is used for parking) and 81.1m high, 40 m x 40 m square in-plane moment resisting steel frame (MRF), with a 15m x 15m in-plan center steel-shear walled core. Typical elevation view and floor plan of the building is illustrated in Fig. 2. The foundation consists of a 1.5m thick mat below the core and a 1.37m thick mat at the perimeter of the building plan that changes on each end with width between 3.4m and 3.7m. The exterior and core mats are interconnected with grade beams (Fig. 3).

Building location belongs to site class D with site amplification factor of about 3.0 at 1 Hz (Dutta et al. 2000; Martirosyan et al. 2002). The site soil profile consists of layered glacial, fluvial, stillwater, and colluvial deposits. The soil profile with shear wave velocity at the AB site is shown in Fig. 4. Extensive investigation has been conducted on this site. Nine boreholes with the depth varying from 12m to 31m were drilled and logged before the construction of the building. Two testing holes were drilled and sampled to test the soil properties in 1981. Seven boreholes have been recently finished at a site close to the building to install the downhole array, with the deepest extending to the depth of 61m. The site can roughly be divided into five layers. The first layer is about 11m thick and consists of poorly graded sand and gravel. The second layer extends from 11m to 21m and is mainly composed of silt and lean clay. The third layer reaches 35m depth and is mainly consists of glacial deposits of interbedded clay, silt and sand, an important Quaternary unit of the Anchorage basin, called the Bootlegger Cove Formation (BCF). This type of soil, with a width of several kilometers, underlies lowland areas in west-central Anchorage, including downtown area, lost shear capacity due to the seismic shaking, resulting in ground failure and a graben in downtown Anchorage during the 1964 Great Alaska Earthquake. Below 35m, the soil is stiff with layered silt, sand and clay. Starting from 52m, older, dense and hard glacial till is observed and extends to the bottom of boring. These represent typical site conditions for downtown Anchorage. Because of the presence of the soft clay layer beneath the building foundation, SSI effects at the AB are expected to be significant and pronounced. Thus, the AB site is an excellent candidate for study of SSI effects.

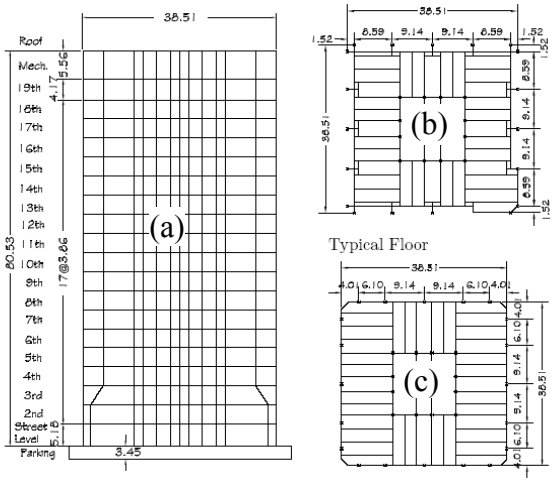

Fig. 2 Typical elevation and plan views of the AB: (a) Elevation (b) Parking Garage (c) Typical Floor.

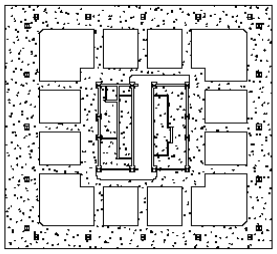

Fig. 3 Sketch of the foundation of the AB.

2.2 The Building and Downhole Instrumentation

The instrumentation of the AB was completed in 2003 under the Advanced National Seismic System (ANSS) program of United States Geological Survey (USGS) (Celebi, 2003; Celebi et al, 2004). The 32-channel seismic sensors (CH 1 – CH 32) are located in the basement garage and on the 1st, 2nd, 7th, 8th, 13th, 14th, 19th, 20th and 21st (roof) floors of the building, as shown in Fig. 5. Among the sensors, there are 29 2g-uniaxial (ES-U) and one tri-axial (ES-T) Force Balance Accelerometers (Episensors of Kinemetrics) with 1.25V/g sensitivity. The ES-T is located at the northwest corner of the basement. As can be seen from Fig. 5, in the parking garage view, there are two vertical accelerometers in the northeast and southwest corners, respectively. These two sensors are able to capture the rocking vibration of the building. As shown in the typical floor view in the same figure, two orthogonal accelerometers (north-south and east-west) are placed at the east side and one accelerometer (north-south) is at the west side of the building at each floor. This configuration is used to record torsional oscillation of the building.

There are three recorders in the data acquisition system, which are housed on the 18th floor of the building. Three telephone lines, each attached with an individual unit, are installed to enable remote access to each of the three recorders. Each recorder is connected with an individual GPS receiver located at the roof of the building, for timing purposes. The recorded signal from each recorder is sampled at 200 samples/sec. The recorders are operated in trigger mode with triggering thresholds varying from 1 gal at the basement to 40 gal at the roof level. The recorder (Recorder #1) connected to the ES-T at the basement has been assigned as the Master unit and is connected with other two recorders (Recorders #2 and #3) by a Master-slave connection.

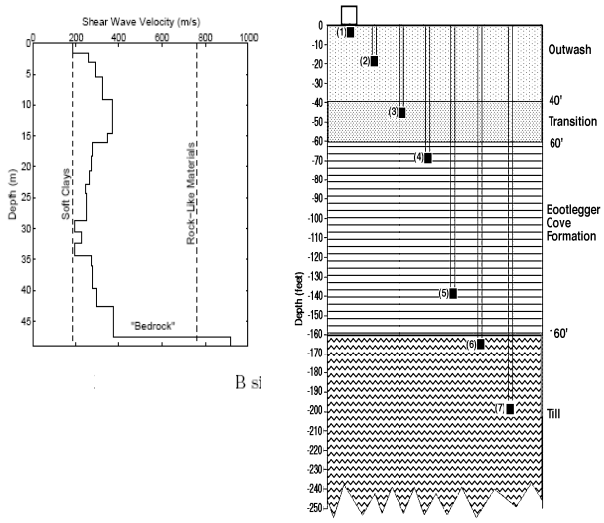

Fig. 4 Soil profile and shear wave

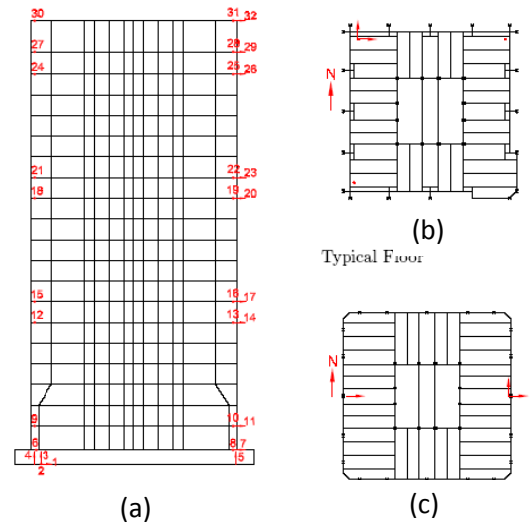

Fig. 5 Accelerometer deployment in AB:
(a) elevation view, looking to the North
(b) parking garage (c) typical floor.

3. System Identification Method-Extended Kalman Filter

3.1 The extended Kalman filter

To describe the application of the extended Kalman filter more completely, here we repeat some important equations.

The general nonlinear state space equation and observation equation can be written as

$$\begin{aligned} x_{k+1} &= f(x_k, u_k, v_k) \\ y_k &= g(x_k, w_k) \end{aligned} \tag{3.1}$$

where k represents the time step, x_k is the state variable, u_k is the input signal driving the state evolution, y_k is the observation variable, v_k and w_k are noises in the state space and observation equations, respectively. All variables can be vectors. f and g are general nonlinear functions. Eq. (3.1) can be linearized around the current state estimate as

$$\begin{aligned} x_{k+1} &\approx f(\hat{x}_k, u_k, \bar{v}_k) + F_x(k)(\bar{x}_k - \hat{x}_k) + F_v(k)(v_k - \bar{v}_k) \\ y_k &\approx g(\bar{x}_k, \bar{w}_k) + G_x(k)(x_k - \bar{x}_k) + G_w(k)(w_k - \bar{w}_k) \end{aligned} \tag{3.2}$$

where $\bar{x}_k$ is the prediction of the state x_k given measurements y_k up to time k-1 (not including the most recent measurement), while $\hat{x}_k$ is the updated estimate of x_k given y_k up to time k

(including the most recent measurement). $\overline{v}_k$ and $\overline{w}_k$ are the expected noise level at time *k*. The linearization coefficients are partial derivatives of the functions f and g with respect to the state and noise variables:

$$
\begin{aligned}
F_x(k) &= \frac{\partial f(x, u_k, \overline{v}_k)}{\partial x}\Big|_{x=\hat{x}_k} \\
F_v(k) &= \frac{\partial f(\hat{x}_k, u_k, v)}{\partial v}\Big|_{v=v_k} \\
G_x(k) &= \frac{\partial g(x, \overline{w}_k)}{\partial x}\Big|_{x=\overline{x}_k} \\
G_w(k) &= \frac{\partial f(\overline{x}_k, w)}{\partial w}\Big|_{w=\overline{w}_k}
\end{aligned}
\tag{4}
$$

The *EKF* algorithm consists of two main steps: (1) an update step where the current state estimate $\hat{x}_k$ is adjusted based on the most current observed data y_k and the previous state prediction, $\overline{x}_k$; (2) a prediction step where the next state $\overline{x}_{k+1}$ is predicted based on the most current state estimate $\hat{x}_k$. These two steps can be expressed in the following equations:

$$
\begin{aligned}
\hat{x}_k &= \overline{x}_k + K_k[y_k - g(\overline{x}_k, \overline{w}_k)] \\
\overline{x}_{k+1} &= f(\hat{x}_k, u_k, \overline{v}_k) + F_x(k)(\overline{x}_k - \hat{x}_k) + F_v(k)(v_k - \overline{v}_k)
\end{aligned}
\tag{5}
$$

where K_k is called as the Kalman gain and can be computed by:

$$
\begin{aligned}
K_k &= \overline{P}(k) G_x(x)^T [G_x(k)\overline{P}(k)G_x(k)^T + G_w(k)R(k)G_w(k)^T]^{-1} \\
\hat{P}(k) &= [I - K_k G_w(k)]\overline{P}(k) \\
\overline{P}(k+1) &= F_x(k)\hat{P}(k)F_x(k)^T + F_v(k)Q(k)F_v(k)^T
\end{aligned}
\tag{6}
$$

here, $R(k)$ and $Q(k)$ are covariance matrices of the noises w_k and v_k, respectively. $\overline{P}(k)$ and $\hat{P}(k)$ are the *predicted* and *updated* covariance matrices, respectively, for the state variable x_k. The *EKF* works by applying the two equations in (5) alternatively and recursively in *k*, thus obtaining the best state estimate for each time step *k* as new observed data become available.

The *EKF* relies on linearization of the state space and observation equations, which requires computation of partial derivatives. Since the computation of partial derivatives can be expensive for complicated nonlinear functions, the *EKF* in the form of Eqs. (5) and (6) may not be suitable for complex nonlinear systems. However, the derivatives can be replaced by finite differences, and a "derivative free" *EKF* can be developed and applied to soil property identification efficiently. This technique is briefly reviewed in the following section.

3.2 The First-Order Polynomial Approximations

Nϕrgaardetc. (2000 a and b) developed polynomial approximations obtained with an interpolation formula for derivatives of state estimators in nonlinear systems. In this method, the estimators become more accurate than those based on Taylor approximations, and yet the implementation is significantly simpler as no derivative computation is required. Thus, it is believed that estimators derived in this way can replace the extended Kalman filter in most practical applications. In this study, first-order polynomial approximations are adopted to replace linearizations of the *EKF* method. The following is a brief description of the "derivative free" first-order polynomial approximations.

The four linearization coefficients in Eq. (3), expressed in Eq. (4) as the partial derivatives of the functions *f* and *g* with respect to the state and noise variables are simplified by the first-order difference approximations. Because all variables are actually vectors, these four coefficients are actually matrixes. They are expressed as (*h* being the difference step):

$$
\begin{aligned}
A_{x\hat{x}}(k) &= \{A_{x\hat{x}}(i,j)\} \\
&= \{(f_i(\hat{x}_k + h\hat{s}_{x,j}, u_k, \bar{v}_k) - f_i(\hat{x}_k - h\hat{s}_{x,j}, u_k, \bar{v}_k))/2h\} \\
A_{xv}(k) &= \{A_{xv}(i,j)\} \\
&= \{(f_i(\hat{x}_k, u_k, \bar{v}_k + hs_{v,j}) - f_i(\hat{x}_k, u_k, \bar{v}_k - hs_{v,j}))/2h\} \\
A_{y\bar{x}}(k) &= \{A_{y\bar{x}}(i,j)\} \\
&= \{(g_i(\bar{x}_k + h\bar{s}_{x,j}, \bar{w}_k) - g_i(\bar{x}_k - h\bar{s}_{x,j}, \bar{w}_k))/2h\} \\
A_{yw}(k) &= \{A_{yw}(i,j)\} \\
&= \{(g_i(\bar{x}_k, \bar{w}_k + hs_{w,j}) - g_i(\bar{x}_k, \bar{w}_k - hs_{w,j}))/2h\}
\end{aligned}
\tag{7}
$$

where the { } represents a single column in the matrix. $A_{x\hat{x}}(k), A_{xv}(k), A_{y\bar{x}}(k), A_{yw}(k)$ and corresponds to $F_x(k), F_v(k), G_x(k)$ and $G_w(k)$ in Eq. (4). The $\bar{s}_x, \hat{s}_x, s_v$ and s_w is the Cholesky factors of the covariance matrixes, respectively. The jth columns of $\bar{s}_x$ and $\hat{s}_x$ are denoted by $\bar{s}_{x,j}$ and $\hat{s}_{x,j}$ respectively, and similarly for other factors. Then $Q, R, \bar{P}$ and $\hat{P}$ in Eq. (6) are defined as follows:

$$
\begin{aligned}
Q &= A_v A_v^T \;;\; R = A_w A_w^T \\
\bar{P} &= \bar{A}_x \bar{A}_x^T \;;\; \hat{P} = \hat{A}_x \hat{A}_x^T
\end{aligned}
\tag{8}
$$

To estimate the state space parameters, we first substitute the coefficients obtained from Eq. (7) into Eq. (8), and then substitute the results of $Q, R, \bar{P}$ and $\hat{P}$ from Eq. (8) into Eq. (6). Subsequently, substitute the results obtained from Eq. (6) into the first part of Eq. (5) to evaluate the values of state parameters of kth step. The state parameters at $(k+1)^{\text{th}}$ step can be obtained from the result at k^{th} step using the second part of Eq. (5). In this way, the state parameters at all steps can be evaluated recursively.

4. Modeling and Identification Procedure

The objective of the project is to develop an identification tool for identifying the structural and site dynamic properties. The research work includes the following tasks:

(a) develop a simplified two-dimensional (2D) shear-bending model for the actual three-dimensional (3D) complicate structure;

(b) develop a numerical interpolation procedure to generate more complete response data for the purpose of structural identification by EKF;

(c) develop a structural identification procedure for the inter-story stiffness of shear type low-rise multi-story structures using the Extended Kalman Filer (EKF) using the single-input multi-outputs approach, using an example of ground-input five-level-outputs;

(d) develop a single-degree-of-freedom (SDOF) uncoupling technique combining with the EKF for the purpose of the identification of inter-story stiffness and damping for high-rise building structures, like AB; and

(e) develop the system identification tool by the EKF for the soil site (bedrock-input downhole-array-outputs conditions) using the recorded data from seismic events at the downhole array of AB.

The detailed modeling and identification procedures are organized in the following Appendixes:

Appendix A
Simplified Two-Dimensional Shear-Bending Structural Model

Appendix B
Method of Displacement Interpolation at Intermediate Non-Instrumented Levels

Appendix C
System Identification of the Inter-Story Stiffness for Shear Type Low-Rise Multi-Story Structures Using the Extended Kalman Filer

Appendix D
System Identification of the Inter-story Stiffness for High-Rise Building Structures Using the Extended Kalman Filer and Recorded Seismic Data

Appendix E
System Identification of Model Parameters for Layered Soils Using the Extended Kalman with the Recorded Seismic Data from the Downhole Array of Atwood Building (AB)

5. Conclusion

The identification procedure developed in this study resolves the problems encountered in applying the MDOF shear model to simulate the multi story and high-rise building structures and layered soil conditions in SSI and site-dependent seismic dynamic response analyses.

The simplified 2D shear-bending model is adopted for AB structural in this study; and the MDOF shear model is adopted to simplify the soil continuous medium. The model parameters are identified by the EKF technique with DD1 procedure using recorded seismic data. The system identification tool was developed for low-rise multi-story and high-rise building structures and layered soil sites. The identification tool can be used for identification of structural dynamic properties of the building like the AB and the soil properties beneath the building. The conclusions from the project include the followings:

(1) Prior to the system identification procedure, a complicated three-dimensional structural model has to be simplified. Therefore, a simplified two-dimensional model of the building AB was developed based on a shear/flexure type structure.

In this study, using a simplified 2D mode for a multistory or a tall building subject to dynamic loads, the AB structure is approximated as linked flexural and shear structures. The approximate method of estimating floor accelerations was applied to calculate displacements along the height of the AB. Good agreement between the recorded and calculated displacements was achieved.

(2) In order to develop a more continuous representation of the response along the height of a multi-story or a tall building, information about the motion of intermediate, non-instrumented floors is desirable. Using recorded accelerations at instrumented floors of the building, the displacements at intermediate floors were interpolated to develop a continuous picture of the motion of the structure along the full height.

The numerical interpolation method using the cubic spline function of displacements for intermediate levels was applied for the AB to obtain a complete input and output data for the EFK identification procedure.

(3) With regarding the system identification tool, first, a method was developed to identify the inter-story stiffness of shear type structures using the extended Kalman filter for the low-rise multi-story structures using the single-input multi-outputs approach; an example of ground-input five-level-outputs was presented.

Using a simplified 2D, the numerical simulation of the EKF procedure was applied to a 5-story building. The results show that the modified EKF can identify the inter-story stiffness and damping efficiently. Because EKF can track the change of model parameters due to structural damage, the modified EKF will be an efficient identification tool for structural health monitoring. Comparing the identified stiffness with the initial structural stiffness, it is possible to evaluate the structural health condition and possible damage in the structure. Based on knowledge of the condition of the structure, certain

preventative measures can be carried out to prolong the service life of the structure and prevent catastrophic failure.

(4) Then, the single-degree-of-freedom uncoupling technique combining with the EKF identification tool was developed for the purpose of the identification of inter-story stiffness and damping for high-rise building structures, like the AB.

A numerical simulation example is given and the comparison between the identified and estimated inter-story stiffness are performed. The effects of noise on the identification results are also discussed. The results showed that the algorithm and the technology presented in this study not only have good identification effectiveness but also have good noise robustness.

(5) Finally, the system identification tool by the EKF for the soil site (bedrock-input downhole-array-outputs conditions) using the recorded data from seismic events at the downhole array of AB was developed.

Using the seismic recorded data from the downhole array, a MDOF shear model was successfully adopted in this study to simulate the behavior of layers soil under earthquake shaking. An iterative procedure was used to modify the initial values. To a certain extent, the procedure can overcome the difficulties in choosing the initial value of parameters in the identification procedure. A fourth-order Runge-Kutta method was used to integrate state equations to improve the accuracy of state estimator. The parameters of the model were identified by the EKF procedure. The results of comparison show that the surface acceleration time history simulated by the identified model parameters are better than that simulated by the initial model parameters using the general engineering estimation method. The results from the identification procedure demonstrate that the EKF procedure is practically suitable method to dealing with the layered soil site in SSI and site-dependent dynamic response analyses.

(6) The EKF procedure developed in this project can be easily adapted to other type structures and soil conditions. As the EKF program matches the recorded outputs, with the inputs, the stiffness, mass and damping properties of the system are identified.

(7) Future study to improve the identification procedure and to apply the recorded data for different structures, buildings, bridges and site conditions, is still required.

The identification approach will play a significant role in the creation of analytical SSI models and in calibration of the Finite Element (FE) models for the structure of AB and its site, in the observation of its site response variations, and in the identification of possible damage to the building or unsatisfactory performance of soil in the future damaging earthquake events.

Appendix A

Simplified Two-Dimensional Shear-Bending Structural Model

Various simplified modeling methods were developed in the 1960s and 1970s for tall buildings. Heidebrecht and Stafford-Smith (1973) derived the closed form solution to the differential equations for a simplified 2D model of a tall building subject to dynamic loads. The structure is approximated as linked flexural and shear beams with uniformly distributed mass and stiffness along the height. A nondimensional coefficient,α, describes the contributions to the displacements from pure flexure and pure shear; $\alpha = 0$ indicating pure flexure, and $\alpha = \infty$ indicating pure shear. The method relied exclusively on response of the 1st dynamic mode.

Miranda (1999) further developed the simplified 2D continuum model for multistory buildings for the purpose of determining displacements for preliminary design of new buildings or rapid evaluation of existing buildings. Modal analysis was incorporated into the method. Miranda (2002) derived equations for nonuniform stiffness along the height of the building. It was found that incorporation of decreasing stiffness along the height of the building has a practically negligible effect on the calculated displacements. Miranda (2002) used the method to study floor accelerations in real buildings responding to real seismic events. Further guidelines were suggested: It was found sufficient to use the first three modes of response for most typical structures, and typical values for α were provided. α between 0 and 1.5 was suggested for shearwalls and braced frames, α between 1.5 and 5 was suggested for buildings with a combination of shearwalls and moment frames, and α between 5 and 20 was given for moment frame buildings.

The approximate method of estimating floor accelerations, as developed by Miranda (2005), was used to calculate displacements along the height of the AB. The Miranda method employs an assumption of continuous mass and stiffness along the height of the building to develop the equation of motion. The method requires calculating the value for the nondimensional parameter,

$$\alpha_o = H * \left(\frac{G * A_o}{E * I_o} \right)^{1/2} \tag{A.1}$$

where H is the building height, G is the shear modulus of the shear walls, A_o is the area of the shearwalls, E is the normal strain modulus for bending, and I_o is the moment of inertia of the bending components. α is a measure of the degree to which the building deflection is defined by pure flexure ($\alpha = 0$) or pure shear ($\alpha = \infty$). According to Miranda, buildings with dual lateral resisting systems of moment resisting frames and braced frames or shear walls typically correspond to $1.5 < \alpha < 5.0$. α can be calculated directly for the building under consideration, typically using the stiffness properties of the lowest building level. For the AB, $\alpha = 2.8$ was calculated for the shear-wall/moment-frame system in the east/west direction. Stiffness reduction along the height of the building was ignored.

The method then requires solution of the characteristic equation for roots corresponding to mode shapes. The first three mode shapes and modal participation factors were calculated based on the mode shape normalized to unity at the top level.

The equivalent modal static response was identified from the response spectra from the basement motion using the identified modal periods. It should be noted that the dynamic response for the first mode is very small relative to the 2nd and 3rd modes. This is due to the ground motion being weak and the absence of lower frequencies. The response to the weak ground motion is dominated by higher modes. Modal displacements were calculated from the equivalent modal static response equation:

$$D_n = \frac{\Gamma_n * \phi_n(x) * a_n}{\omega_n^{\ 2}} \tag{A.2}$$

$$\Gamma_n = \frac{\int_0^1 \phi_n(x)dx}{\int_0^1 \phi_n(x)^2 dx} \tag{A.3}$$

where n is the model number, D_n is the modal displacement, a_n is the spectra pseudo-acceleration, and Γ_n is the modal participation factor. Modal Participation factors for the AB computed from a previously developed three-dimensional Finite Element model are listed in Table A.1:

Table A.1 Modal Participation factors

Mode Number	Modal Participation Factors	East-West	North-South
1	Γ_1	1.471	1.471
2	Γ_2	-0.761	-0.761
3	Γ_3	0.494	0.494

Pseudo-acceleration for each mode from the response spectra of the small earthquake is listed in Table A.2:

Table A.2 SDOF acceleration for each mode from response spectra

Mode Number	Pseudo-acceleration	East-West	North-South
1	a_1 (cm/sec^2)	0.8	0.5
2	a_2 (cm/sec^2)	35.0	25.0
3	a_3 (cm/sec^2)	50.0	35.0

For the design consideration, the damping ratios used for individual modes are listed in Table A.3:

Table A.3 Damping ratios for individual modes:

Mode Number	Damping Ratio	East-West	North-South
1	ξ_1	5%	5%
2	ξ_2	5%	5%
3	ξ_3	5%	5%

Square root sum of squares (SRSS) was selected to combine the peak modal responses, represented by the solid lines in Fig.s A.1 and A.2.

$$D = \sqrt{\sum_{1}^{m} (D_n)^2} \tag{A.4}$$

Maximum positive and negative recorded relative displacements are plotted at each floor level against the calculated displacement. Good agreement between the recorded and calculated displacements was achieved. Maximum variation is less than 0.1 cm and occurs at levels 6 and 7. Fig. A.1 displays East-West displacement. The solid line shows the calculated maximum position; and the samples represent the maximum position from the recorded or interpolated data. The recordings are taken at the center of mass. Fig. A.2 displays the North-South displacement recordings taken at the East and West sides of the building. There is some difference between the maximum displacements at each floor level, indicating that the AB is subject to torsional motion.

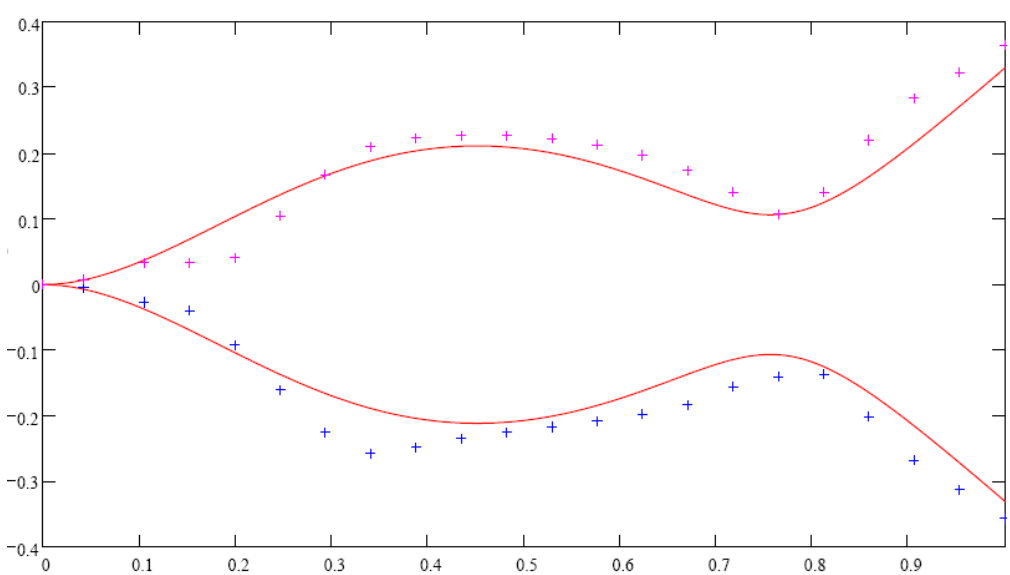

Fig. A.1: East-West Displacement (Relative)

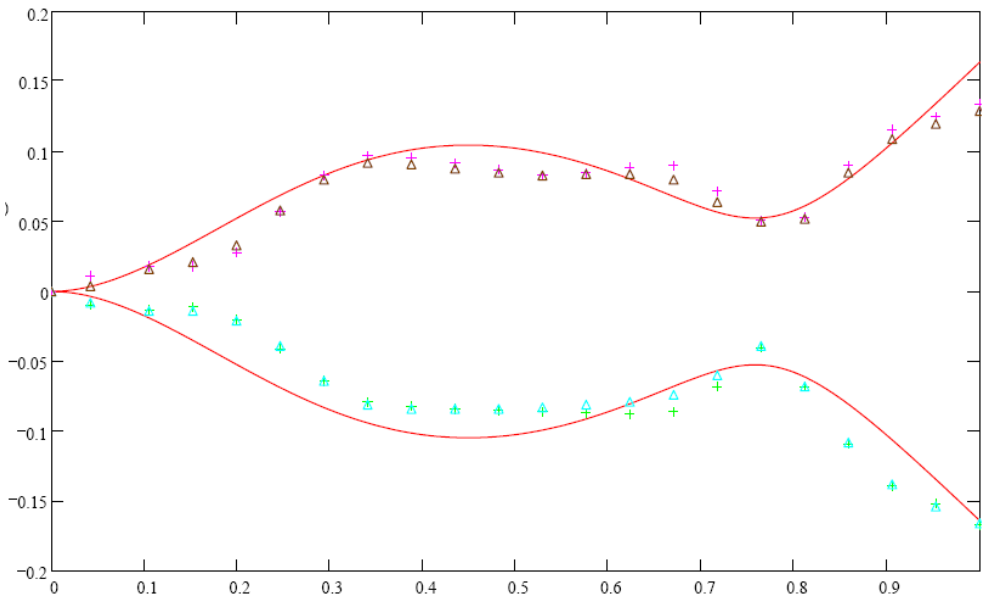

Fig. A.2: North South Displacement (Relative)

Next, acceleration time history for individual floors was predicted by the simplified method:

$$\ddot{u}(x,t) \cong \ddot{u}_g(t) + \sum_{i=1}^{m} \Gamma_i \phi_i(x) \ddot{D}_i(t) \qquad \text{(A.5)}$$

Good agreement between the recorded and predicted values was achieved and is plotted in Fig. A.3 for the Roof and Fig. A. 4 for 13th level. The small differences between the recorded and calculated displacements can be attributed to simplifications present in the 2-D model, and to the use of only the first three mode shapes.

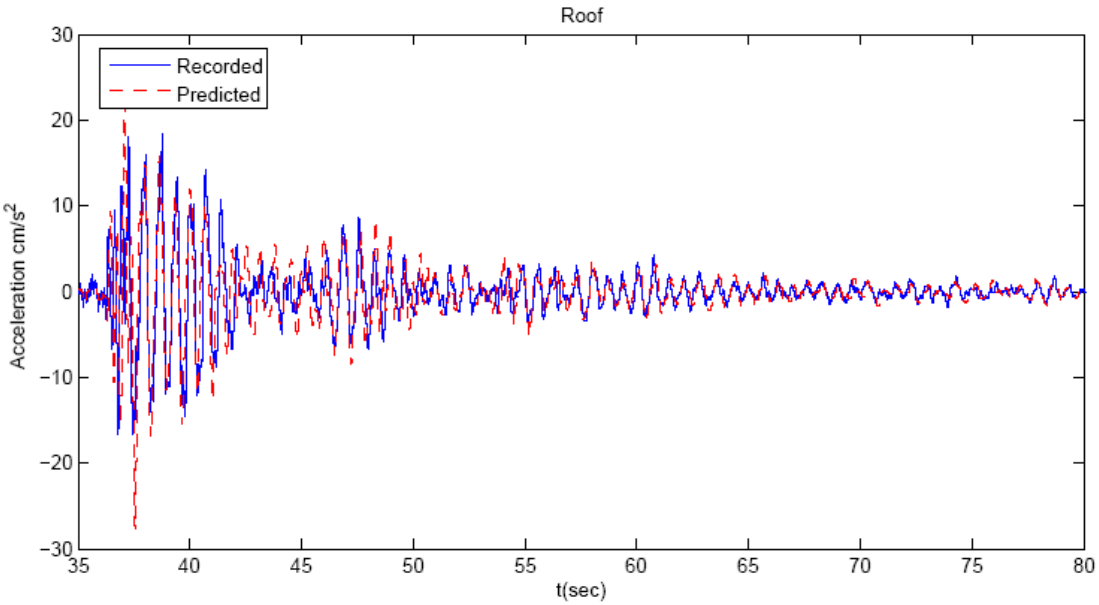

Fig. A.3: Roof Acceleration (Relative).

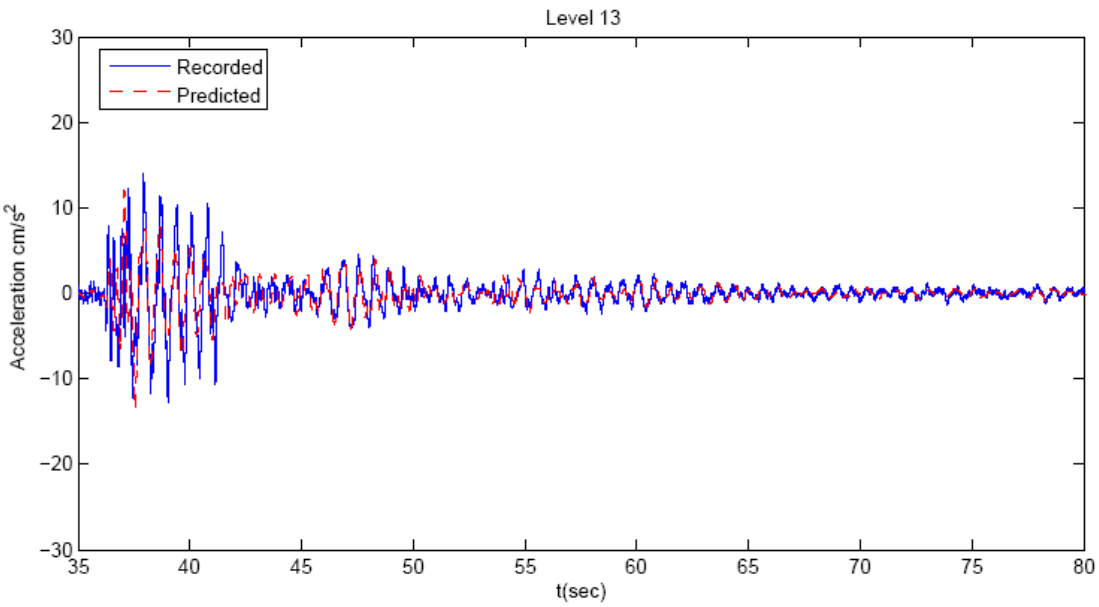

Fig. A. 4: Acceleration (Relative) for 13th level.

Appendix B

Method of Displacement Interpolation at Intermediate Non-Instrumented Levels

In order to develop a more continuous representation of the response along the height of the building, information about the motion of intermediate, non-instrumented floors is desirable. De La Llera and Chopra (1998) developed a method using cubic spline interpolation of displacements for intermediate levels. This method was used for the AB. Total acceleration was recorded at instrumented levels: basement, 1st, 2nd, 7th, 8th, 13th, 14th, 19th, 20th and roof. Total displacements were calculated by integrating the total acceleration data twice. The relative displacements at instrumented levels were produced by subtracting the displacement at the basement level. Relative displacements at non-instrumented levels (3rd, 4th, 5th, 6th, 9th, 10th, 11th, 12th, 15th, 16th, 17th and 18th) were interpolated by a cubic spline function using MATLAB. Relative accelerations were then calculated by twice differentiating the displacements. The flow chart of the procedure is shown in Fig. B.1.

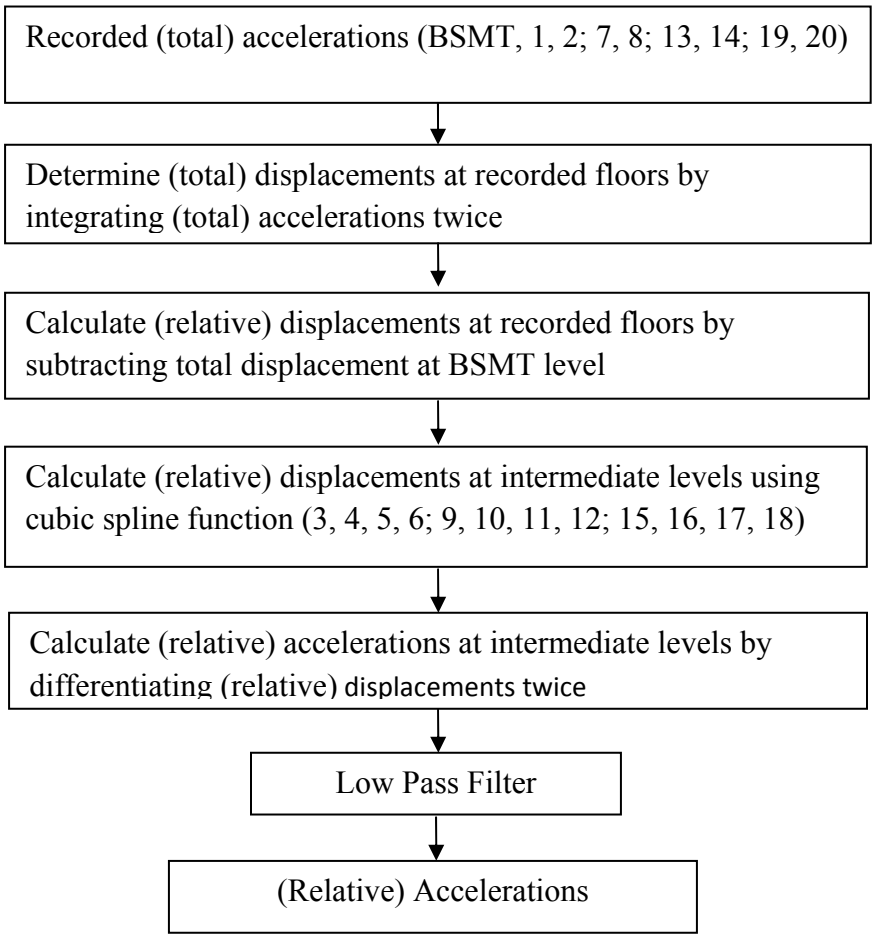

Fig. B.1: The flow chart of the interpolation

Fig. B.2 shows an example of the recorded and interpolated data for an earthquake.

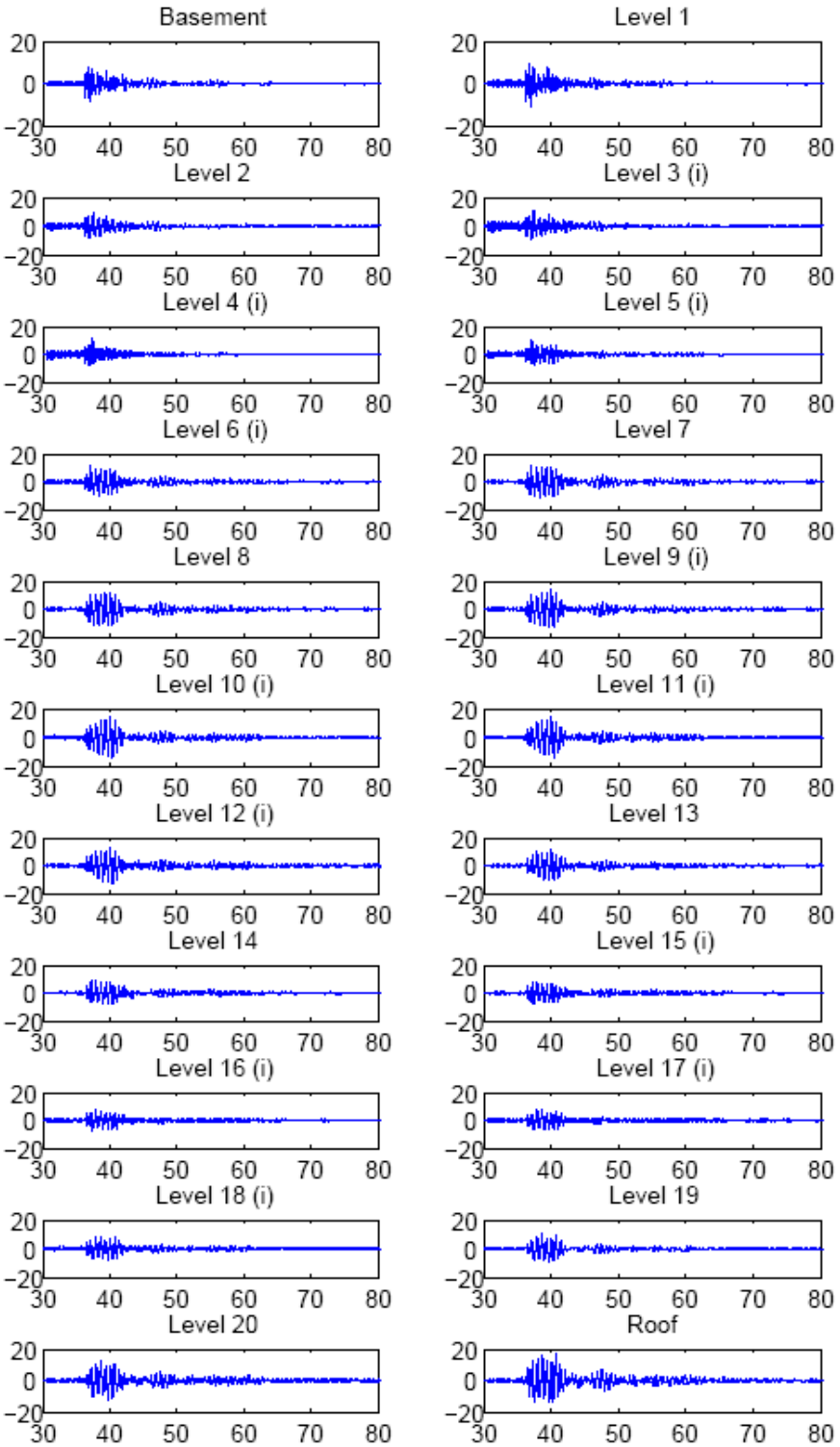

Fig. B.2: Recorded and Interpolated Accelerations

In Fig. B.2, the horizontal axes are “Time” with unit of second; and the vertical axes are “Recorded or Interpolated Acceleration” data with unites of cm/s/s.

Using the interpolated acceleration response data in the following EKF identification procedure, the complete the input and output data are available.

Appendix C

System Identification of the Inter-Story Stiffness for Shear Type Low-Rise Multi-Story Structures Using the Extended Kalman Filer

The paper, "Identification of the inter-story stiffness of shear type structures using the extended Kalman filer", was published at the "World Forum on Smart Materials and Smart Structures Technology" Chongqing & Nanjing, China, May 22-27, 2007

Authors: He Liu, Mansheng Wang, Yibin Zheng and Xiyuan Zhou

See the paper in a separate file.

Appendix D

System Identification of the Inter-story Stiffness for High-Rise Building Structures Using the Extended Kalman Filter and Recorded Seismic Data

D.1 Introduction

In this project, the direct identification approach is applied for high-rise buildings. We propose an adaptive tracking technique, based on the EKF approach, to identify structural parameters, inter-story stiffness and damping, and their variations with time in case of possible nonlinear structural response during an earthquake for high-rise buildings.

A numerical simulation example is given and the comparison between the identified and estimated inter-story stiffness are performed. The effects of noise on the identification results are also discussed. The results showed that the algorithm and the technology presented in this study not only have good identification effectiveness but also have good noise robustness.

To describe the identification procedure and numerical example easily, in the following discussion, a typical 20 story shear-bending building structure is the assumed identification target.

D.2 Identification Procedure

The identification procedure includes follows:

(1) The structure was simulated as a mass-spring-damper system. The degree-of-freedom (DOF) was reduced from the original several thousands in a three-dimensional (3D) Finite Element analysis (FEA) model into 20 DOF in a two-dimensional (2D) model, namely each DOF for each floor.

(2) It was assumed that the accelerometers were only deployed at 10 floor levels; therefore the recorded data were incomplete. The necessary seismic response data in other 10 stories without accelerometers were generated using the numerical interpolations.

(3) A decoupling algorithm for the simultaneous equations of motion of the mass-spring-damper system was applied to the mass-spring-damper system. The advantages of the algorithm are simple, fast-solving and highly accurate.

(4) The extend Kalman filter (EKF) was used in this study because of its applicability to nonlinear time-varying processes. The input signals used in the EKF procedure were recorded accelerations at the accelerometer-station in the ground level; whereas the output signals were “recorded” (see detail in the following example) and interpolated seismic response signals at the 20 floor levels.

(5) To improve the computational efficiency and accuracy, the first-order polynomial approximations for derivation of state estimators was applied in the EKF procedure. Because of the advantages of using polynomial approximations obtained with an interpolation formula for derivation of state estimators, the estimators are more accurate than estimators based on Taylor approximations, and yet the implementation is significantly simpler as no derivatives are required.

D.3 Decoupling Algorithm for the Mass-Spring-Damping System

In the 2D shear-bending structural model, the floor masses are represented by concentrated masses, the lateral inter-story stiffness and damping are represented as springs and dampers as shown in Fig. D.1. For this structural model, considering only one horizontal degree of freedom, the mass, damping and stiffness matrixes can be simplified and expressed as follows:

$$M = \begin{bmatrix} m_1 & 0 & 0 & \dots & 0 & 0 \\ 0 & m_2 & 0 & \dots & 0 & 0 \\ \dots & \dots & \dots & \dots & \dots & \dots \\ 0 & 0 & 0 & \dots & m_{n-1} & 0 \\ 0 & 0 & 0 & \dots & 0 & m_n \end{bmatrix}$$

$$C = \begin{bmatrix} c_1 & -c_1 & 0 & \dots & 0 & 0 & 0 \\ -c_1 & c_1 + c_2 & -c_2 & \dots & 0 & 0 & 0 \\ \dots & \dots & \dots & \dots & \dots & \dots & \dots \\ 0 & 0 & 0 & \dots & -c_{n-2} & c_{n-2} + c_{n-1} & -c_{n-1} \\ 0 & 0 & 0 & \dots & 0 & -c_{n-1} & c_{n-1} + c_n \end{bmatrix}$$

$$K = \begin{bmatrix} k_1 & -k_1 & 0 & \dots & 0 & 0 & 0 \\ -k_1 & k_1 + k_2 & -k_2 & \dots & 0 & 0 & 0 \\ \dots & \dots & \dots & \dots & \dots & \dots & \dots \\ 0 & 0 & 0 & \dots & -k_{n-2} & k_{n-2} + k_{n-1} & -k_{n-1} \\ 0 & 0 & 0 & \dots & 0 & -k_{n-1} & k_{n-1} + k_n \end{bmatrix}$$

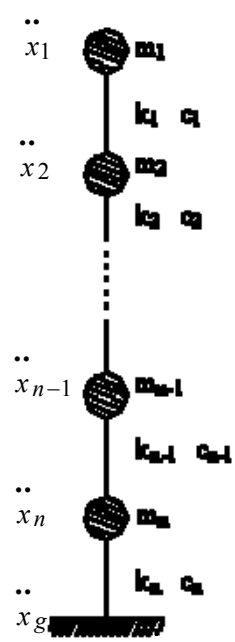

Fig. D.1: Mass-Spring

Its equations of motion due to ground motions can be expressed as

$$M\ddot{X} + C\dot{X} + KX = -MI\ddot{x}_g \qquad \text{(D.1)}$$

where X is relative displacement, with respect ground, vector of masses at floor levels; $\dot{X}$ and $\ddot{X}$ are corresponding velocity and acceleration vectors, respectively; I is the unit vector and $\ddot{x}_g$ is the ground acceleration time function in the horizontal direction.

Defining x_i is the absolute horizontal displacement of m_i and $x_{n+1} = x_g$, then, the relative displacement x_{ij} between masses i and j can be represented as：

$$X = [x_1 - x_{n+1}, \quad x_2 - x_{n+1}, \quad \cdot \quad \cdot \quad \cdot \quad , \quad x_n - x_{n+1}]^{\mathrm{T}}$$
$$x_{ij} = x_i - x_j = x_{ig} - x_{jg}$$

Based on these relationships, Bao et al (1990) developed equations of motion for the multi-degree-of-freedom (MDOF) mass-spring-damping system as

$$m_l \ddot{x}_{l,l+1} + c_l \dot{x}_{l,l+1} + k_l x_{l,l+1} = -m_l \ddot{x}_{l+1} - \sum_{j=1}^{l-1} m_j \ddot{x}_j \ , \quad l = 1,2,...,n \qquad \text{（D.2）}$$

and validated the equations by the mathematic induction approach.

Reorganizing Eq. (D.2), we can get

$$m_l \ddot{x}_{l,l+1} + c_l \dot{x}_{l,l+1} + k_l x_{l,l+1} = -m_l [\ddot{x}_{l+1} - (\sum_{j=1}^{l-1} m_j \ddot{x}_j)/m_l] \ , \quad l = 1,2,...,n \qquad \text{（D.3）}$$

Using the simplified notation

$$\ddot{x}_{gl} = [\ddot{x}_{l+1} - (\sum_{j=1}^{l-1} m_j \ddot{x}_j)/m_l] ; \quad x_{l,l+1} = x_{le} ,$$

the Eq. (D.3) can be rewritten as

$$m_l \ddot{x}_{le} + c_l \dot{x}_{le} + k_l x_{le} = -m_l \ddot{x}_{gl} \ , \quad l = 1,2,...,n \qquad \text{（D.4）}$$

where $\ddot{x}_{gl}$ represents the equivalent seismic acceleration of the mass l and x_{le} the differential displacement response between the mass l and $l+1$ due to the corresponding equivalent seismic force.

If the masses and the corresponding equivalent seismic responses are known, the Eq. (D.4) is completely uncoupled. It means that the seismic response of the MDOF mass-spring-damping system can be decomposed into the responses from a multi single-degree-of-freedom (SDOF) system under the same equivalent seismic excitation force. It can be seen easily that the decoupling calculation reduces the computation effort significantly.

D.4 Extended Kalman filter for the Decoupled SDOF system

Based on Eq. (D.4), we can define the state variable matrix as

$$S = [s_1 \qquad s_2 \qquad s_3 \qquad s_4]^T \tag{D.5}$$

where $s_1 = x_{le}$, $s_2 = \dot{x}_{le}$, $s_3 = k_l$, $s_4 = c_l$.

Therefore, the Eq.'s (D.4) can be rewrite as

$$\dot{S} = \begin{Bmatrix} \dot{s}_1 \\ \dot{s}_2 \\ \dot{s}_3 \\ \dot{s}_4 \end{Bmatrix} = \begin{Bmatrix} s_2 \\ -s_4 s_2 / m_l - s_3 s_1 / m_l - \ddot{x}_{gl} \\ 0 \\ 0 \end{Bmatrix} = F(S,t) \tag{D.6}$$

The Eq.'s (D.6) are nonlinear state equations of the state variables. We can rewrite them as a dispersed equation, Eq. (D.7), and add the observation equations, Eq. (D.8), as

$$\dot{S}_k = F(S_k, t_k) \tag{D.7}$$

$$\{x_{le}\}_k = h(S_k, t_k) + \{v\}_k \tag{D.8}$$

where $h(S_k, t_k)$ is the observation function vector, and v is a random observation noise vector with zero mean.

By linearization around the filtered estimating values, that means, using the incremental linear equations instead of the original nonlinear equations in a sampling time interval, the state functions of a system by extended Kalman filter (Li et al, 2002) can be obtained as follows.

<u>State estimation equation:</u>

$$\tilde{S}_{k+1} = \hat{S}_k + \int_{t_k}^{t_{k+1}} F(\hat{S}_k, t_k) dt \tag{D.9}$$

where $\hat{S}_k$ is estimated state value of S_k at time interval k, and $\tilde{S}_{k+1}$ is expected state value of S_{k+1} at time interval $k+1$.

<u>State transfer matrix:</u>

$$\Phi_k = e^{A(\hat{S}_k)\Delta t} \approx I + \Delta t \cdot A(\hat{S}_k) \tag{D.10}$$

where $A = [\frac{\partial F_i(\hat{S}_k)}{\partial \hat{s}_j}]$. A_{ij} represents the derivative of the ith component of function F with respect to the jth component of variable s_j; I is the unit matrix; and Δt is the sampling interval.

Error covariance expectation equation:

$$\tilde{P}_{k+1} = \Phi_k P_k \Phi_k^T \qquad \text{(D.11)}$$

Augment matrix:

$$K_{k+1} = \tilde{P}_{k+1} H_{k+1}^T (H_{k+1} \tilde{P}_{k+1} H_{k+1}^T + R_{k+1})^{-1} \qquad \text{(D.12)}$$

where $H_k = [\frac{\partial h_i(\hat{S}_k)}{\partial \hat{s}_j}]$. R is the covariance matrix of the observation noise v.

State filter equation:

$$\hat{S}_{k+1} = \tilde{S}_{k+1} + K_{k+1}[\{x_{le}\}_{k+1} - h(\tilde{S}_{k+1})] \qquad \text{(D.13)}$$

Error covariance filter equation:

$$P_{k+1} = (I - K_{k+1} H_{k+1}) \tilde{P}_{k+1} \qquad \text{(D.14)}$$

D.5 Simulation Example

It was assumed that a 20 story shear-bending type building which could be simulated as a mass-spring-damper chain system with 20 DOF as shown in Fig. D.1. Also it was assumed that the structural story masses were known as shown in Table D.1 and D.2. The purpose of the structural identification was to estimate the inter-story stiffness and damping.

In this simulation example, the ground motion was assumed as the Taft earthquake and the recorded structural responses at 10 stories were assumed as the calculated structural response. In the EKF identification procedure, the inter-story stiffness and damping are nonlinear parameters to be identified; however, for the purpose of generating the simulated structural time-history response, as so called "recorded data", we had to pre-assume the inter-story stiffness and damping for the structure. The assumed inter-story stiffness is shown in Table D.1.

For the structural damping properties, it was assumed that inter-story damping follows Rayleigh damping assumption with mass proportional coefficient 0.2 and stiffness coefficient

0.0125. In addition, it was assumed there were 10 accelerometers deployed at 10 levels with locations shown in Table D.2. In Table D.1 and D.2, i is the order of the story levels from top down with i=1 showing the roof level and i=21 showing the ground level. The check marks in Table D.2 indicate the instrumented levels. Since the observed data, namely the "recorded" structural response, were not complete, we used the limited observed response data at the 10 levels (for i=1, 2, 3, 8, 9, 14, 15, 19, 20 and 21, note that the data at level 21 were recorded ground motion input) to estimate the missing response at other levels (for i=4, 5, 6, 7, 10, 11, 12, 13, 16, 17 and 18) through numerical interpolation by cubic spline function.

Table D.1 Structural mechanical parameters

i	1	2	3	4	5	6	7	8	9	10
m_i (T)	130.6	208.1	208.1	208.1	208.1	208.1	208.1	208.1	208.1	208.1
k_i (KN/M)	20700	34000	34000	34000	34000	34000	34000	34000	34000	34000
i	11	12	13	14	15	16	17	18	19	20
m_i (T)	208.1	208.1	208.1	208.1	208.1	208.1	208.1	224.5	268.4	284.7
k_i (KN/M)	34000	34000	34000	34000	34000	34000	34000	35000	36400	45000

Table D.2 Deployment of accelerometers

i	1	2	3	4	5	6	7	8	9	10	11	12	13	14	15	16	17	18	19	20	21
	√	√	√					√	√					√	√				√	√	√

As aforementioned, the ground input motion was assumed as the Taft earthquake with duration 60 seconds, sampling rate 0.02 second. Fig. D.2 shows the recorded acceleration time history of Taft earthquake.

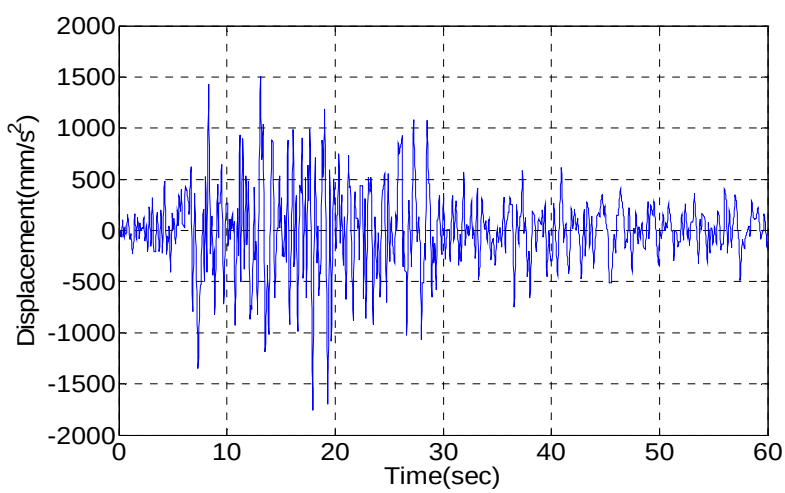

Fig. D.2: Acceleration time history of Taft earthquake

First, we used the numerical dynamic analysis to obtain the structural time history response for the stories with accelerometers deployed (for i=1, 2, 3, 8, 9, 14, 15, 19 and 20). Then, we used these response data to estimate the structural response at the stories without accelerometers (for i=4, 5, 6, 7, 10, 11, 12, 13, 16, 17 and 18) by numerical interpolation via cubic spline function. Thus, we got the complete observation data for the EKF identification. Fig. D.3 and D.4 show the true response acceleration time histories and estimated via interpolation at mass levels 5 and 8, respectively.

The inter-story damping was also identified. The results are sensitive to the initial assumed values. Additional work on the damping identification is required in the future study.

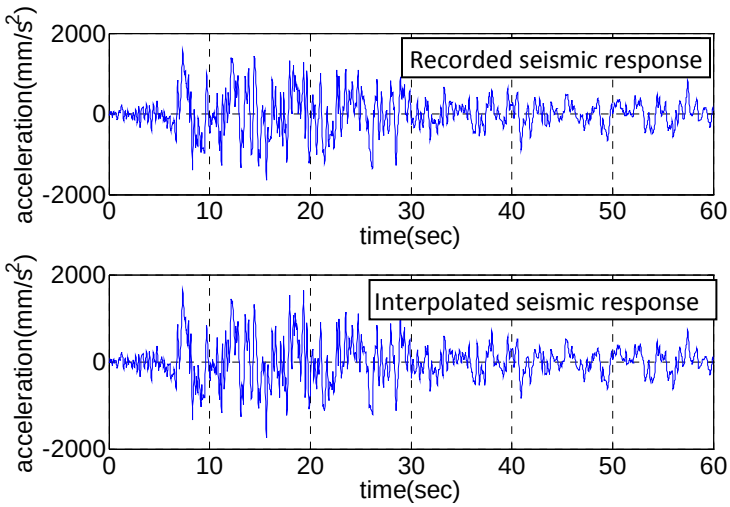

Fig. D.3: Comparison of actual acceleration time history with the estimated interpolation results at the mass level 5.

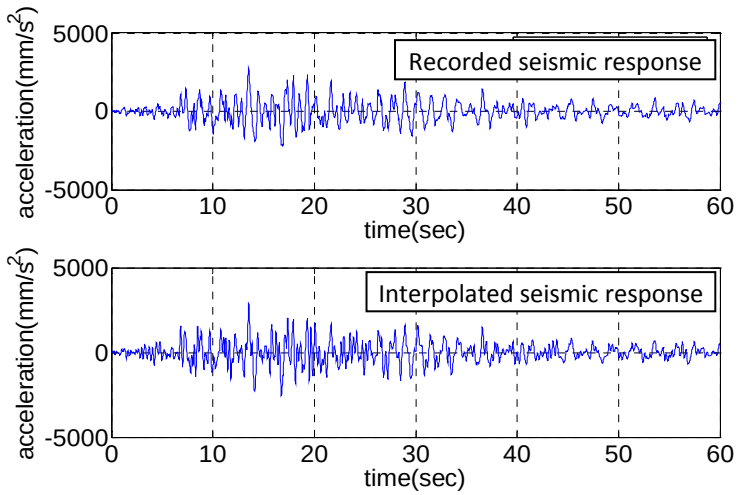

Fig. D.4: Comparison of actual acceleration time history with the estimated interpolation results at the mass level 8.

Using the aforementioned uncoupled SDOF algorithm and the EKF identification procedure, we got the identified inter-story stiffness and damping. The resulting inter-story stiffness is shown in Table D.3. In Table D.3 the error is defined as

$$Identification \quad Error = \left| \frac{Identified\,value - Actual \quad value}{Actual \quad value} \right| (100\%) \tag{D.15}$$

Table D.3 Inter-story stiffness and its error

i	1	2	3	4	5	6	7	8	9	10
Identified k_i (KN/M)	20481	33697	34650	34203	33935	33752	33644	33519	33927	33994
Error	1.06%	0.89%	1.91%	0.60%	0.19%	0.73%	1.05%	1.41%	0.21%	0.02%
i	11	12	13	14	15	16	17	18	19	20
Identified k_i (KN/M)	33954	33807	33361	33136	32932	33582	35493	39109	43664	59310
Error	0.14%	0.57%	1.88%	2.54%	3.14%	1.23%	1.41%	7.44%	2.97%	1.15%

From Table D.3 it can be seen that the maximum error in the inter-story stiffness is about 7.44% whereas most of errors are less than 3%. Considering the identification procedure was based on estimated interpolation of structural response at 11 mass levels, we can believe that the identification procedure is stable, reliable and the results are acceptable for engineering applications. If the complete structural response data are available, the expected errors should be less.

Practically the actual recorded data are always with noise, whereas the assumed calculated structural responses are without the noise. To simulate the actual effects of the noise on the identification results, we added the artificial noise onto the structural response data for both the "recorded" from 9 levels and the "interpolated" at 11 levels. The noise was generated by normal distributed white noise with zero mean as shown below

$$\tilde{\ddot{R}}_k = \ddot{R}_k (1 + r_k \cdot p) \tag{D.16}$$

Where $\ddot{R}_k$ and $\tilde{\ddot{R}}_k$ are structural responses at time step k before and after adding the noise, respectively. r_k is a normal distributed random variable with zero mean and unit standard deviation. p is the noise level. In this example, the noise level was determined as 10% which represented a very strong noise interfere.

Using the structural response data including the 10% noise as observed signal in the EKF procedure, we re-did the identification. The resulting inter-story stiffness is listed in Table D.4. It

can be seen that except the top two stories, the errors of inter-story stiffness in most stories are less than 7.5 %.

Table D.4 Inter-story stiffness and its error with strong noise interfere

i	1	2	3	4	5	6	7	8	9	10
Identified k_i (KN/M)	13973	28614	33857	31504	31985	33229	31971	33949	31476	35554
Error	32.5%	15.84%	0.42%	7.34%	5.93%	2.27%	5.97%	0.15%	7.42%	4.57%
i	11	12	13	14	15	16	17	18	19	20
Identified k_i (KN/M)	33948	33635	32213	32892	32553	33573	35771	39003	43679	59310
Error	0.15%	1.07%	5.26%	3.26%	4.26%	1.26%	2.20%	7.15%	2.94%	1.15%

D.6 Conclusion

For online identification of the inter-story stiffness and damping of high-rise structures during an earthquake event, a series of algorithms was adopted: the EKF technology, the first-order polynomial approximation, the simplified shear-bending type 2-D structure, the decoupling algorithm of equation of motion for the mass-spring-damper chain system and the cubic spline interpolation. A test of numerical simulation to the algorithms was carried out with the noise interference considered in the observation data. The identification results were comparatively satisfied.

The series of algorithms for the identification are reliable and valuable for practical engineering.

Appendix E

System Identification of Model Parameters for Layered Soils Using the Extended Kalman with the Recorded Seismic Data from the Downhole Array of Atwood Building

E1. Introduction

The catastrophic aftermath of several recent earthquakes in different parts of the world has posed a serious challenge to the structural engineers to understand critically various aspects of the seismic performance of soil-structure interaction (SSI) systems. Various simulation models for SSI systems are developed. There are two main approaches for analyzing SSI, namely the direct method and substructure method (Wolf, 1985, 1988). In substructure method, many researchers developed simple mechanical models with only limited number of degrees-of-freedom for soils (Wolf J. P., 1985; Wolf J. P. and Somaini D. R., 1986; De Barros F. C. P. and Luco J. E., 1990; Luan M. and Lin G., 1995). Among the available mechanical models for soils in SSI and site-dependent dynamic response analyses, the shear type multi-degrees-of-freedom (MDOF) model for layered-soils is well-known in time-domain analysis, because it has good trade-off of accuracy and simplicity (Xie, 1987).

There is much literature on how to determine the parameters of these shear type mechanical models for layered-soils. However, all of the available methods are based on experienced assumptions. As for realistic layered-soils or complex site, it is impossible to determine the actual parameters of simple mechanical models by experienced assumptions. To identify the associated model parameters, we suggest applying the modified Extended Kalman Filter (EKF) in this project to identify the equivalent parameters in layered soil conditions because of its applicability to nonlinear time-varying processes. (Zheng et al, 2004; Liu et al, 2005; Wang et al, 2003).

In current years, downhole arrays have been operated in many places to provide essential seismic data for studying the effects of local soil conditions. Downhole arrays are an efficient tool for seismic analyses of site response and amplification. For this reason, the recorded seismic data from the downhole array of AB are used in this study to identify the model parameters.

In this project, we apply the system identification method based on the extended Kalman filter (EKF) with *DD1* (first-order approximation divided difference) to determine the inter-layer parameters for the shear type MDOF model. A realistic identification example is given for the soil site of AB using the available recorded seismic data from the downhole array. To improve the accuracy of state estimator in the EKF procedure, we use the fourth-order Runge-Kutta method to integrate the state equations. An iterative process is also developed in this project to create more meaningful initial parameters. The results of the example demonstrate the feasibility and practicality of the proposed identification technique.

The shear type MDOF model can be used in time-domain nonlinear analysis of SSI for layered or complex soil conditions. The identified parameters of layered-soils can improve the calculating accuracy of seismic analysis involving SSI and site-dependent dynamic response. It

is also shown from this project that the simulation models can be better identified by the instrumental measurements from the recorded seismic data.

The identification technique developed in this paper provides a useful basis for analyzing SSI and site-dependent seismic response analysis for uniform or layered soils. If the mechanical model of the super-structure is available, the complete model of the coupled soil-structure system can be constructed by assembling the super-structure model and the shear type soil model.

E2. Multi-degrees-of-freedom shear model and its application to layered soil

The MDOF shear type model is adopted to simulate the soil dynamic characteristics in this study. Fig. E.1 shows the MDOF shear model for layered-soil in consideration. The following assumptions are made for the shear type model in this project:

(1) The soils are considered as horizontally uniformly layered. A soil "column" with unit cross-sectional area in each layer is extracted from the site to represent the layered soil in infinite large area.

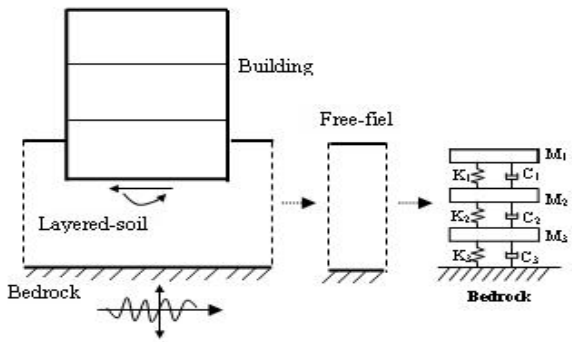

Fig. E.1: MDOF shear model for layered-soil

(2) Assume that the horizontal, vertical and rocking vibrations of soil layers are independent each other, that is, the coupling effects among the horizontal, vertical and rocking vibrations are negligible. For the layered-soil in the study, only the horizontal vibration is considered.

(3) The mass in each layer is assumed lumped at the top surface of the layer.

(4) Inter-layer shear stiffness and damping coefficient of each layer in the soil "column" are represented by a spring and a dashpot.

(5) The interface between the soil column and the bedrock is horizontal without a slope.

In this model, each layer consists of one oscillator mass, one spring, and one dashpot as shown in Fig. E.1. The equations of motion of the MDOF shear model can be written as

$$M\ddot{U} + C\dot{U} + KU = P \tag{E.1}$$

where, M, C, K are the mass, damping and stiffness matrixes, respectively; U and P are displacement and excitation force vectors, respectively, expressed as follows:

$$M = \begin{bmatrix} m_1 & & \\ & \ddots & \\ & & m_n \end{bmatrix}; \quad C = \begin{bmatrix} c_1 & -c_1 & & & & \\ -c_1 & c_1 + c_2 & -c_2 & & 0 & \\ & & \ddots & & & \\ & 0 & & -c_{n-2} & c_{n-2} + c_{n-1} & -c_{n-1} \\ & & & & -c_{n-1} & c_{n-1} + c_n \end{bmatrix} \tag{E.2a}$$

$$K = \begin{bmatrix} k_1 & -k_1 & & & & \\ -k_1 & k_1 + k_2 & -k_2 & & 0 & \\ & & \ddots & & & \\ & 0 & & -k_{n-2} & k_{n-2} + k_{n-1} & -k_{n-1} \\ & & & & -k_{n-1} & k_{n-1} + k_n \end{bmatrix} \tag{E.2b}$$

$$\mathrm{U} = [\mathrm{u}_1 \quad \cdots \quad \mathrm{u}_\mathrm{n}]^\mathrm{T}; P = \left[-m_1 \ddot{u}_r \quad \cdots \quad -m_n \ddot{u}_r\right]^T \tag{E.2c}$$

where $\ddot{u}_r$ is the input earthquake acceleration at the bedrock.

This shear type model provides simplicity, however, not accuracy for the following reasons:

(1) Actual conditions of the soil site are not pure horizontally layered; rather, the geotechnical conditions are much complex comparing with aforementioned layered model.

(2) The soil material and dynamic properties are very complicated, showing non-layered, heterogeneity, anisotropy and nonlinearity, which can't simply be represented by a spring and dash pot.

(3) The soil site is continuous medium with mass distributed and varied in three dimensions. The soil can be seen as the physical medium connecting the super-structure and the bedrock. The identification procedure should reflect the transmission of seismic energy among the bedrock, subsoil and super-structure. The concentrated mass assumption may cause a significant error in the modeling and numerical calculation. Since an earthquake induces the propagation of seismic waves through the continuous soil medium, the lumped mass, spring and dashpot system can't simulate the main features of the dynamic properties of soil body properly.

E3. Identification of the parameters of MDOF shear model using recorded seismic data

E3.1 Input and observation data

In this study, the single-input and multi-outputs identifying technique is used. The earthquake acceleration records at the bedrock were used as single-input signal and at the each layered-soil (at downholes) as observation signals.

E3.2 The state equation and the observation equation

When we apply the EKF with *DD1* to identify the parameters of MDOF shear model using recorded seismic data, the model can be described by a non-linear state space equation and an observation equation. Both equations can be linearized using the "derivative free" technique described in the previous section. In this study, the parameters of the soil model are considered as the state parameters of the system. Specifically, the state vector can be defined as,

$$X^T = [x_1(t), \dot{x}_1(t), \cdots, x_n(t), \dot{x}_n(t), m_1, k_1, c_1, \cdots, m_n, k_n, c_n] \tag{E.3}$$

where, $x_1(t), \dot{x}_1(t), \cdots$ are displacements and velocities of oscillators $m_1, \cdots$ in the soil mechanical model, respectively, $m_1, k_1, c_1, \cdots$ are the parameters of layered-soil in the model, respectively. The nonlinear state equation of model can be expressed as follows,

$$\dot{X}^T = [\dot{x}_1(t), \ddot{x}_1(t), \cdots, \dot{x}_n(t), \ddot{x}_n(t), 0, 0, 0, \cdots, 0, 0, 0]. \tag{E.4}$$

In Eq. (E.4), the acceleration vector of all oscillators in the model can be calculated using the Eq. (E.1),

$$\begin{aligned}
\ddot{x}_1(t_k) &= -m_1^{-1}[k_1(x_1(t_k) - x_2(t_k)) + c_1(\dot{x}_1(t_k) - \dot{x}_2(t_k)) + m_1\ddot{u}_r(t_k)] \\
\ddot{x}_2(t_k) &= -m_2^{-1}[k_1(x_2(t_k) - x_1(t_k)) + k_2(x_2(t_k) - x_3(t_k)) \\
&\qquad + c_1(\dot{x}_2(t_k) - \dot{x}_1(t_k)) + c_2(\dot{x}_2(t_k) - \dot{x}_3(t_k)) + m_2\ddot{u}_r(t_k)] \\
&\vdots \\
\ddot{x}_n(t_k) &= -m_n^{-1}[k_{n-1}(x_n(t_k) - x_{n-1}(t_k)) + k_n x_n(t_k) \\
&\qquad + c_{n-1}(\dot{x}_n(t_k) - \dot{x}_{n-1}(t_k)) + k_n\ddot{u}_r(t_k)] \\
\ddot{u}_r(t_k) &= \ddot{u}_r(t_k) + v(t_k)
\end{aligned} \tag{E.5}$$

where $\ddot{u}_r(t_k)$ is the input earthquake acceleration at the bedrock and $v(t_k)$ is the noise of input earthquake signal. Note that although all parameters of the soil mechanical model are assumed constant *a priori* in the state equation, their estimates are allowed to vary with time in the EKF with DD1 procedure. The displacement and velocity responses of all oscillator $m_1, \cdots$ were used as the observation vector with observation noise $w_i(t_k)$ (i=1, 2). The observation equation is then,

$$g(t_k) = \begin{bmatrix} x_1(t_k) + w_1(t_k) \\ \dot{x}_1(t_k) + w_2(t_k) \\ \vdots \\ x_n(t_k) + w_{2n-1}(t_k) \\ \dot{x}_n(t_k) + w_{2n}(t_k) \end{bmatrix} \qquad k = 1, 2, \ldots, N \ . \tag{E.6}$$

where N is the number of samples, $g(t_k)$ is the observation vector at $t_k = kdt$. The state vector in Eq. (E.3) can be integrated by using the state equation (E.4). In this study, the state equations (E.4) are integrated using a fourth-order Runge-Kutta method, which is a commonly used and stable numerical integration method. Moreover, when integrate equations (E.4) by Runge-Kutta; we don't consider any assumptions, such as, the constant acceleration assumption. From Eq. (E.3), one can see that the output signals in the state equation are velocity and displacement. Since the earthquake recorded data are accelerations in general, it is necessary to numerically integrate the acceleration data to obtain the corresponding velocity and displacement prior to the identification procedure.

E3.3 Initial values of state victors

The number of identified parameters of state vectors in the system depends on number of soil stratums in the site. Convergence to a reasonable estimate may not be obtained if the initial guess is too poor or if the perturbations are so large that the linearization is inadequate to describe the system. To determine the initial values of state victors, the method to estimate the parameters of MDOF shear type model in literatures (Xie, 1987; Shou et al, 1982) was used.

The initial displacement and velocity were calculated based on the integration of acceleration from the downhole array at the end of the first time step $t=dt$ for oscillators $m_1, \cdots m_n$. The spring stiffness of each layered-soil can be estimated by the simplified formula

$$K_i = G_i / h_i \tag{E.7}$$

where G_i and h_i are the shear modulus ($G_i = \rho_i V_{si}$) and the depth of each layered soil stratum, respectively. The damping coefficient can be assumed as Rayleigh damping

$$C_i = \omega\lambda M_i + \frac{\lambda}{\omega} K_i \tag{E.8}$$

where ω and λ are the predominant frequency and the damping ratio (assumed as 5% to all soil stratums) of realistic site respectively. In this study, an approximate formula of the site predominant frequency

$$\omega = \frac{2\pi}{T_s} = \frac{2\pi V_s}{4H} \tag{E.9}$$

was used, based on the site profile of shear wave velocity.

The initial values of the covariance of state parameters may also affect the identification results. In this study, an iterative procedure was used to improve the approximation of all of initial values (see Fig. E.2).

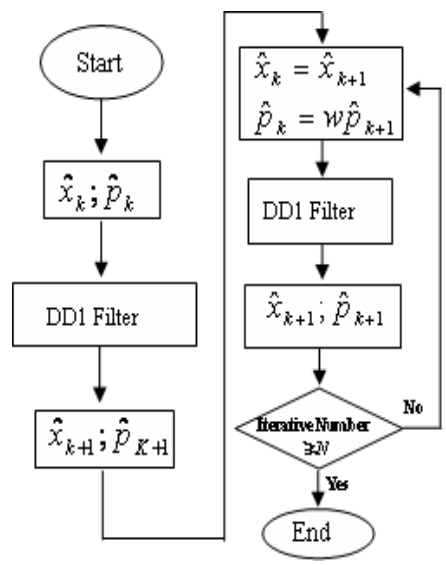

Fig. E.2: Weight iterative

Because the iterative procedure can adjust the rough initial values of parameters more close to the actual values, the 'adjusted' initial values will improve the identified accuracy and stability in the DD1 filter identification procedure. In this study, using the iterative procedure, the estimated values of state parameters and covariance at time step t_{k+1} were used as the new initial values and then the state parameters were re-identified at time step t_{k+1} until convergence was reached. In general, the number of iterative loops can be chosen as a small number when initial values of parameters and covariance are reasonably chosen. In Fig. E.2, the symbol w (in general, more than 1) is the weight of estimated covariance in order to expand the area of estimation of state parameters. Since the identification technique is robust, the initial values do not need very close to the "true" values. It is demonstrated from the example in the following section that as long as the initial values in the similar order of magnitude, the identification procedure will adjust the variables recursively and converge to the "best fit" values quickly and stably.

E4. Identification example

The identification procedure is illustrated in the following example. The AB office building is located in downtown Anchorage. The subsoil under the foundation is roughly divided into five major layers according to the site soil profile. Shear wave velocity profile at the site is shown in Fig. E.3. The first layer is about 10 m thick and consists of poorly graded sand and gravel. The second layer extends from 10 m to 17 m and is mainly composed of silt and lean clay. the third layer reaches 48 m and is mainly composed of soft, locally sensitive clay and silty clay, which belongs to Bootlegger Core Formation (BCF).

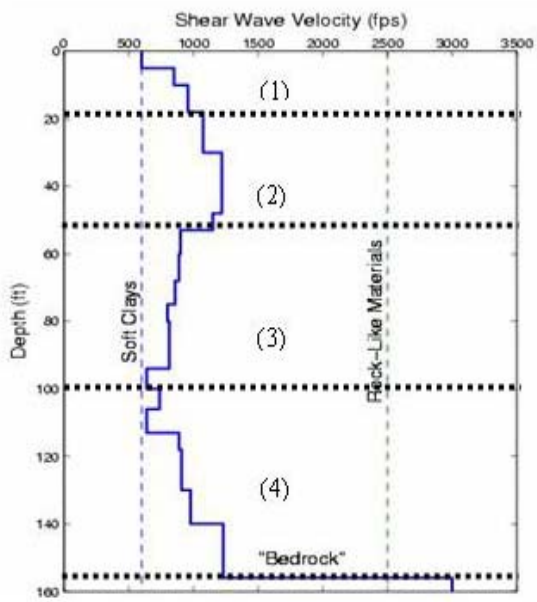

Fig. E.3: Shear wave velocity of the

In order to improve the accuracy of model, the third layer soil is divided into two stratums based on the shear wave velocity (see Fig. E.3). Below 48 m, the soil becomes very stiff with layered silt, sand and clay. The older, dense and hard glacial till is encountered below 55 m, which extends to the bottom of drilled hole. The downhole array (see Fig. E.4) is located at about 100 m south of the AB in the Delaney Park. The array includes six tri-axial strong motion sensors located at the bottom of six boreholes of 3 to 68 m depths. In addition to this, the array also includes one tri-axial surface sensor. The real time data acquisition system of the array consists of four high dynamic range digital recorders.

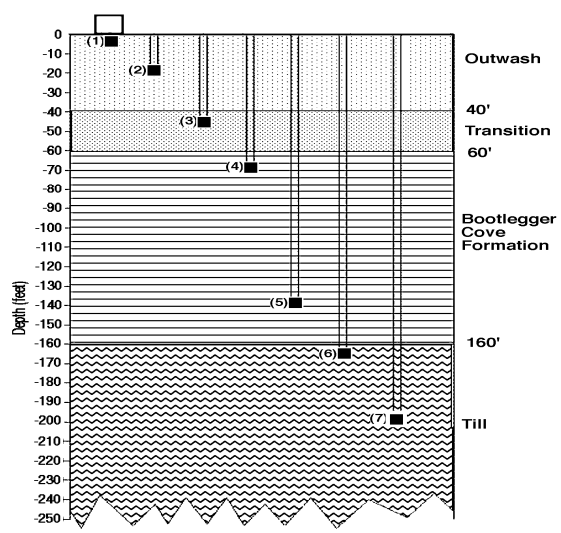

Fig. E.4: Downhole array profile

The array has been operational since September 2004. (He Liu et al 2006). The deepest sensor located in the glacial till formation has shear wave velocity more than 900m/s, corresponding to engineering bedrock. In this study, the recorded acceleration at this level was used as the system input. In Fig. E.4, the numbers 1-7 denote the sensors at different depths. It should be pointed out that the number 6 sensor did not work when the seismic event (used in this study) happened. 4-layers shear model was created to simulate the site, in which the seismic data from sensor 7 were used as the input and the seismic data from sensor 1, 3, 4 and 5 were the output for the first to fourth layer of the shear model, respectively. The reason to choose recorded data at sensor 1, 3, 4 and 5 as the output signals is because these sensors are almost located at the top of layered soil stratums, which are corresponding to the location of mass for each layer.

The February 16, 2006 Earthquake in Alaska (*M*=4.7, 35 *km* depth at Anchorage distance of 14 *km*) was chosen as the seismic event in this study. The peak ground acceleration at downhole near the AB was about 12.15 cm/s^2. The accelerometers at the downhole stations recorded motions in three orthogonal directions including vertical and two orthogonal horizontal directions. The data sampling rate in the accelerometers was 200 samples per second. For the recording duration of 120 seconds, the total computational steps were 24,000. From Fig. E.5, it can be seen that the seismic P-wave arrived at about 30th second and the S-wave at 36th second, respectively. The acceleration and displacement time histories in the HNE direction from the downholes and free surface are shown in Fig's E. 5 and E. 6, respectively. The velocity and displacement time histories of the oscillators in the model were obtained by integrating the recorded acceleration signals. The output displacement time histories in the HNE direction are shown in Fig. E.6.

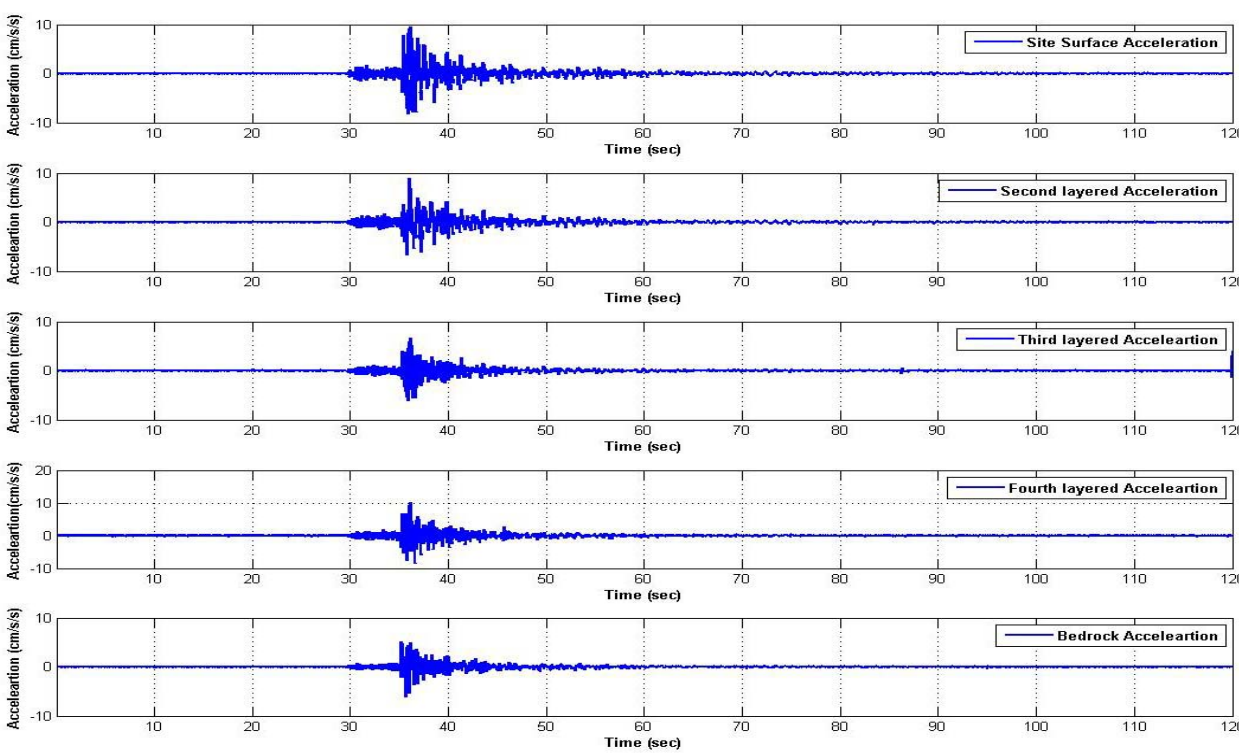

Fig. E.5: Acceleration time histories in the HNE direction recorded at the downhole array

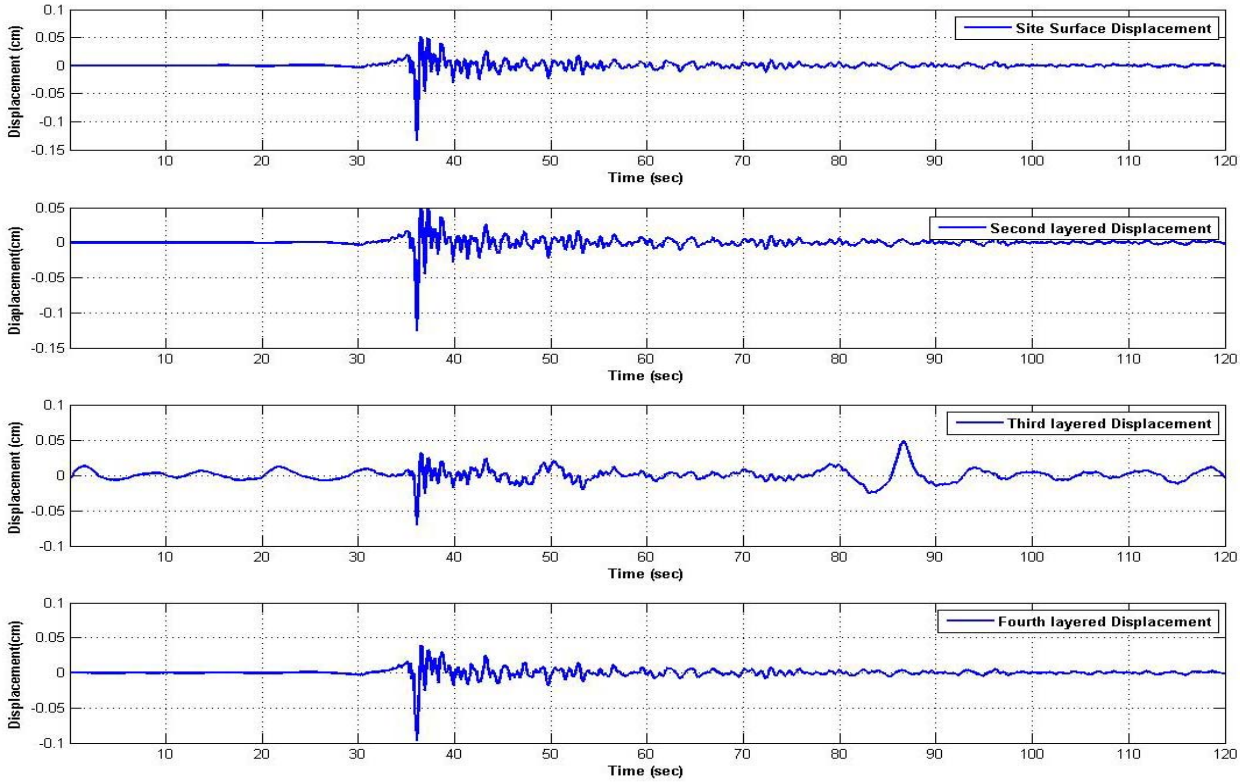

Fig. E.6: Displacement time histories in the HNE direction integrated from the accelerations

The initial parameters, vectors and the covariance matrix of the state space variables need to be determined as described as aforementioned. The convergent paths of all the parameters in the model are shown in Fig. E.7. The initial and identified results of the model parameters in the HNE direction are shown in Table E.1. It can be seen in Fig. E.7 that the identified parameters vary with time mainly start from the time of S-wave arrival, that is about 36th second after recording data. As expected, there were differences between the initial and the identified values, especially in the mass quantities. It is also observed that the recursion procedure is very stable. In this example, the parameters converge to almost constants and do not exhibit obvious further variation with time, indicating that the earthquake shaking was quite weak and the soil behavior was apparently linear.

Table E.1 Initial and identified results of the model parameters.

Parameter	First layer			Second layer		
	M_1 (kg)	K_1 (kN/m)	C_1 (kN-S/m)	M_2 (kg)	K_2 (kN/m)	C_2 (kN-S/m)
Initial Value	1.372650 e+004	2.196240 e+007	1.101522 e+005	1.690990 e+004	3.744753 e+007	1.843496 e+005
Identified Final Value	1.101997 e+004	2.194391 e+007	1.174604 e+005	1.141795 e+004	3.742653 e+007	1.874575 e+005
Parameter	Third layer			Fourth layer		
	M_3 (kg)	K_3 (kN/m)	C_3 (kN-S/m)	M_4 (kg)	K_4 (kN/m)	C_4 (kN-S/m)
Initial Value	2.450840e +004	5.461997e +006	3.865890e +004	3.501168e +004	1.701575e +007	9.835928e +004
Identified Final Value	1.215573e +004	5.527112e +006	4.486154e +004	4.482056e +004	1.696716e +007	1.039582e +005

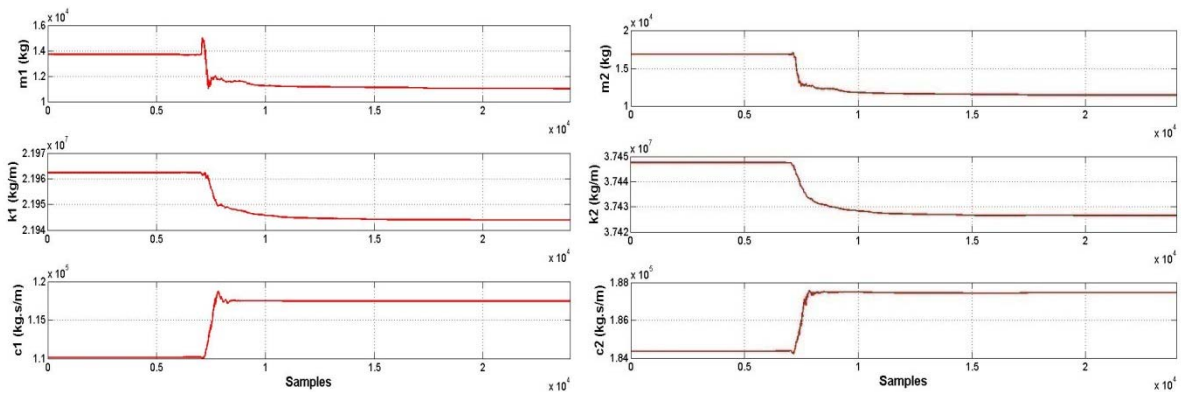

(a) Variation of the parameters in the first layer (left) and the second layer (right)

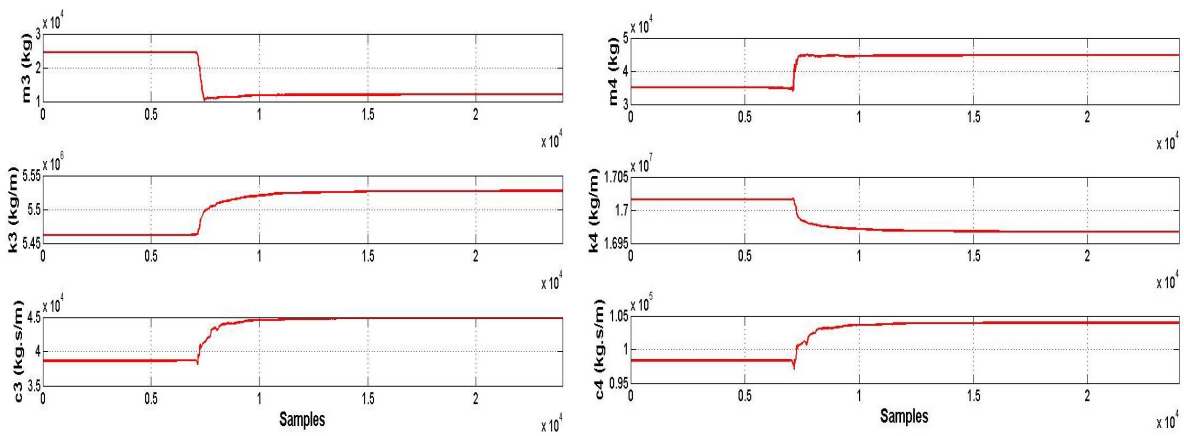

(b) Variation of the parameters in the third layer (left) and the fourth layer (right)

Fig, E.7: Evolution of the identified parameters in the model.

Fig. E.8 shows the comparison of observed (from the recorded data) and identified displacement time histories of all oscillators in the model. A good agreement in the displacement time histories between the observed from the recorded data and the identified via the EKF procedure can be found.

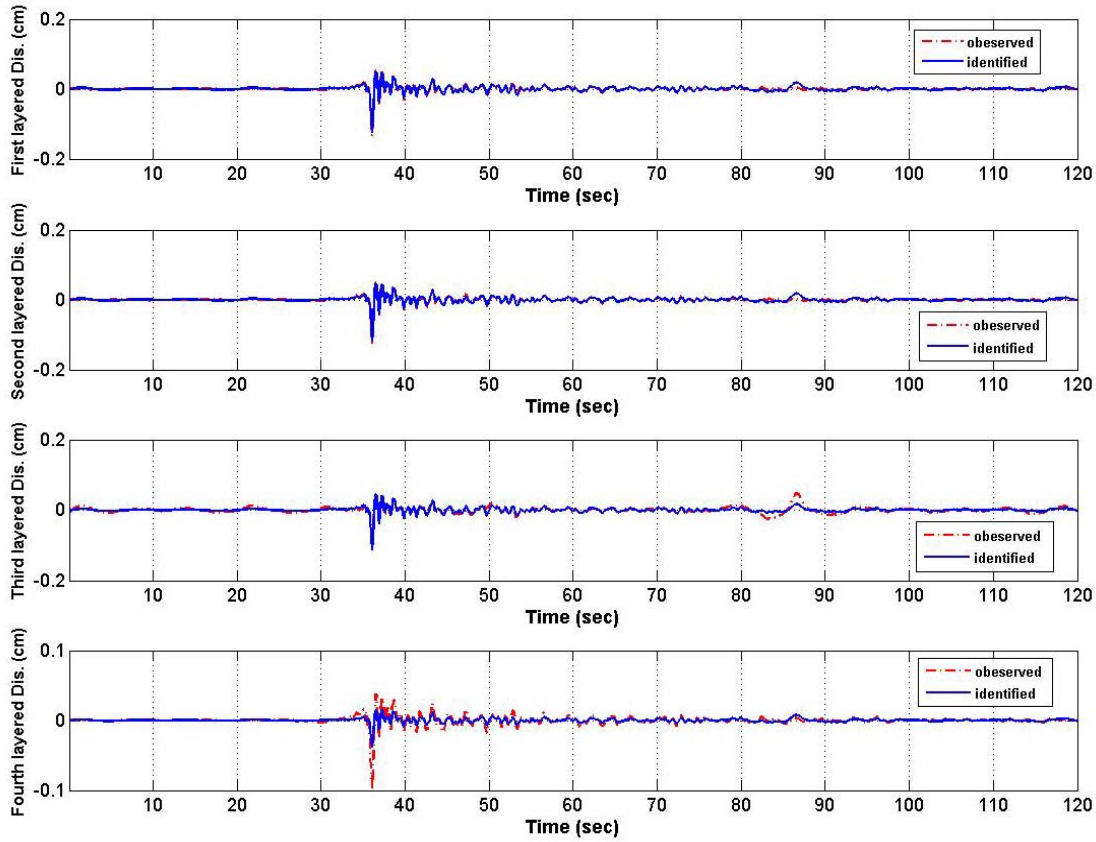

Fig. E.8: Comparison of displacement time histories in the HNE direction

In this example, all identified parameters converged quickly and remained stationary. These results demonstrate that identification accuracy is efficient and reliable when the EKF method is combined with the first-order polynomial approximation technique.

E5. Verification of identified results

Since the soil response was mainly linear during the seismic event in the previous example, we may compare the identified results in time and frequency domains with other available methods. For this purpose, we first simulate the seismic wave propagation from the bedrock to the surface using the initial and identified MODF shear model by Wilson-θ integration method using the recorded acceleration at bedrock is used as input. Fig. E.9 shows the comparison of the surface seismic acceleration between the recorded data and the simulated results by the initial and identified MODF shear model, respectively. It can be seen, in Fig. E.9, that the simulated acceleration time history from the identified model parameters more close to that from the initial model values. The simulated acceleration time history from the identified parameters has the closed peak value with the recorded; and the peak values of both accelerations occur at the same

time. The comparison demonstrates that the identified model is more reasonable than the initial model to simulate layered-soil dynamic characteristics.

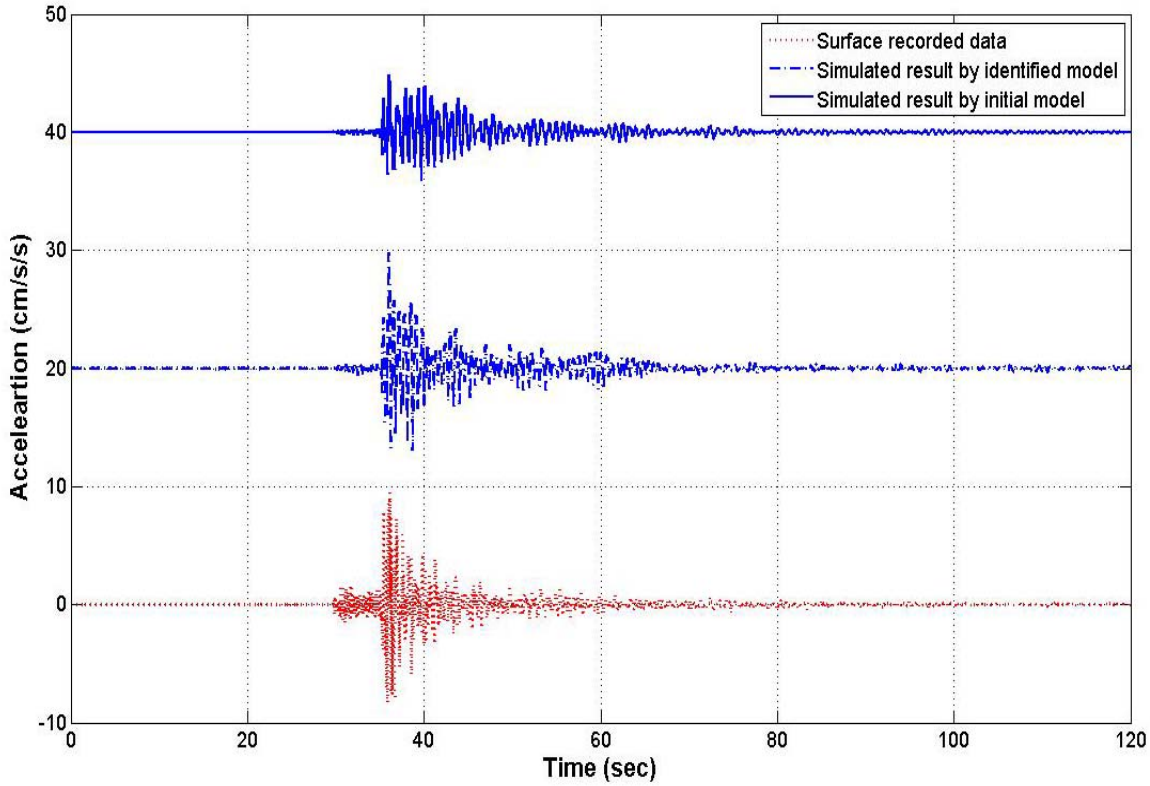

Fig. E.9: Comparison of recorded and simulated acceleration time histories in HNE direction.

The site prominent frequency is estimated as 10.68 Hz by using the approximate formula ($\omega = \frac{2\pi}{T_s} = \frac{2\pi V_s}{4H}$) based on the shear wave velocity profile, where V_s is an average shear wave velocity of the site. If the site prominent frequency is calculated from the MODF shear model, the result is 10.29 Hz by using the identified parameters and 8.23 Hz by using the initial parameters. Therefore, the identified parameters are more trustworthy than the initial parameters using the general engineering estimation method.

Although the MDOF shear model is simple and acceptable for preliminary study in practical applications, the model is naturally with too many assumptions as aforementioned, which may not satisfy the actual conditions. For example in this study, the soil condition is more complex with the overall "layers" not uniform and the surface of bed rock not horizontal. This significantly simplified model may cause the identified results not accurately reflecting the site dynamic characteristics. Further study in the modeling technique is necessary.

E6. Conclusions

The MDOF shear model is adopted in this study to simplify the soil continuous medium. The model parameters are identified by the EKF technique with DD1 procedure using recorded seismic data. The identification procedure developed in this study resolves the problems encountered in applying the MDOF shear model to simulate layered soil conditions in SSI and site-dependent seismic dynamic response analyses. The following are specific conclusions drawn from this study:

1. The MDOF shear model was successfully adopted in this study to simulate the behavior of layers soil under earthquake shaking. The parameters of the model were identified by the EKF procedure. The results from the identification procedure demonstrate that the EKF procedure is a powerful and reliable technique in the application of identification of soil dynamic parameters.

2. The first-order polynomial approximations are adopted to replace the linearization of the *EKF* method. In this derivative-free method, the estimators become more accurate than that based on Taylor approximations, and yet the implementation is significantly simpler as no derivative computation is required.

3. Using the seismic recorded data from the downhole array to identify the soil parameters of the MODF shear model is practically suitable method to dealing with the layered soil site in SSI and site-dependent dynamic response analyses.

4. The practical example using the realistic seismic recorded data demonstrates the efficiency of the identification technique for layered soils. The results of comparison show that the surface acceleration time history simulated by the identified model parameters are better than that simulated by the initial model parameters using the general engineering estimation method.

5. An iterative procedure was used to modify the initial values. To a certain extent, the procedure can overcome the difficulties in choosing the initial value of parameters in the identification procedure. A fourth-order Runge-Kutta method was used to integrate state equations to improve the accuracy of state estimator.

6. The MDOF shear model is significantly simpler than actual complex soil conditions. The model assumptions may cause the identified results not accurate. Further study in the modeling technique is necessary.

References

ASCE Standard (2003), "Minimum Design Loads for Buildings and Other Structures", SEI/ASCE 7-02, Second Edition.

Bao et al (宝志雯, 史文月) (1990), "基于推广卡尔曼滤波算法的结构模型的参数识别", Journal of 振动与冲击 1990(1): 11-21 (in Chinese).

Celebi, M. (2000), "Seismic Instrumentation of Buildings", Open-File Report 00-157, USGS, April.

Çelebi, M.(2003), "Seismic Instrumentation Plan for Robert B. Atwood Building, Anchorage, AK 99501., Administrative Report, United States Geological Survey.

Çelebi, M., McCarthy, J., Biswas, N., Wald, L., Page, R., and Steidl, J. (2004), Seismic Monitoring of the Atwood building in Anchorage, Alaska, USGS, FS2004-3103 (http://pubs.usgs.gov/fs/2004/3103/)

Çelebi, M. (2005), "Integrated seismic monitoring of the Atwood Building, Anchorage (AK) and recorded Earthquake responses", CD-ROM PROC of 8th US National Conference on Earthquake Engineering, San Francisco, CA., April 2006,

Çelebi, M. (2006), "Recorded Earthquake Responses from the Integrated Seismic Monitoring Network of the Atwood Building, Anchorage, (AK)", (accepted-in print) Earthquake Spectra.

Chopra, A. K., and Goel, R.K. (2004), "A modal pushover analysis procedure to estimate seismic demands for unsymmetric buildings", Earthquake Engineering Structural Dynamics, 33(8) 903-927.

Chopra, A. (2001), Dynamics of Structures: Theory and Application to Earthquake Engineering, Prentice-Hall.

De Barros F C P., Luco J E., "Discrete Models for Vertical Vibrations of Surface and Embedded Foundation," Earthquake Engineering and Structural Dynamics, 1990, 19: pp 289~303.

Dutta, U., Biswas, N., Martirosyan, A., Nath, S., Dravinski, M., Papageorgiou, A., and Combellick, R., (2000), "Delineation of spatial variation of shear wave velocity with high-frequency Rayleigh waves in Anchorage", AK, Geophys. J. Intl., 143, 365-375.

Holmes, W. (2000), "The 1997 NEHRP Recommended Provisions for Seismic Regulations for New Buildings and Other Structure", Earthquake Spectra, Volume 16, Issue 1, pp. 101-114.

Li et al (李杰, 李国强) (2002), "工程结构动力检测理论与应用". Science and Technolory, Beijing, 2002: 153-159 (in Chinese).

Liu, H., Yang, Z., Scott, W., Kono, T. and Dutta, U.,"Structural Identification and Modeling of an Instrumented 20-story Atwood Building in Anchorage, Alaska". Proceedings of the 2005 Joint ASME/ASCE/SES Conference on Mechanics and Materials, Baton Rouge, LO, June 1-3, 2005.

Liu, H., Zheng, Y., Wang, M., Yao, Y. and Zhou, X.,(2005), "Time-Domain Identification of Nonlinear Dynamic Property of Foundation Soil due to Seismic Excitation", Proc. of the 2005 Joint ASME/ASCE/SES Conference on Mechanics and Materials, June 1-3, 2005 Baton Rouge, Louisiana.

Luan, Maotian and Lin, Gao, (1995), "Two-degree-of-freedom Lumped Parameters Model of Dynamic Impedances of Foundation Soils," Journal of Dalian University of Technology，1995, Vol. 36. No: 4, pp 477~481 (in Chinese).

Martirosyan, A., Dutta, U., Biswas, N., Papageorgiou, A. and Combellick, R., "Determination of site response in Anchorage, AK, based on spectral ratio methods", Earthq. Spectra, 2002.

NEHRP (2003), "NEHRP Recommended Provisions for Seismic Regulations for New Buildings and Other Structures", Federal Emergency Management Agency, FEMA 450-1/2003 Edition.

Nφrgaard M, Poulsen N K and Ravn O (2000 a), "Advances in Derivative-Free State Estimation for Nonlinear Systems," *Technical Report*: *IMM-REP-1998-15*, Department of Mathematical Modeling, Informatics and Mathematical Modeling, Technical University of Denmark (DTU), 1998, (revised Apr. 2000).

Nφrgaard M, Poulsen N K and Ravn O (2000 b), "New Developments in State Estimations for Nonlinear Systems," *Automatic* (36:11), Nov.:1627-1638.

Wilson, E., "Three Dimensional Static and Dynamic Analysis of Structures", a publication of Computers and Structures, Inc., 1996.

Wolf, J. P. (1985), "*Dynamic Soil-Structure Interaction*," England wood Cliffs, NJ. Prentice Hall.

Wolf, J. P. and Somaini, D. R. (1986), "Approximate Dynamic Model of Embedded Foundation in Time Domain," *Earthquake Engineering and Structure Dynamics*, 14: 683~703. Heidebrecht, A, Stafford-Smith, B. (1973), "Approximate analysis of tall wall-frame structures", Journal of the Structural Division, ASCE, 99(2), 199-221.

Miranda, E., (1999), "Approximate seismic lateral deformation demands in multistory buildings", Journal of Structural Engineering, April 1999, 417-425.

Miranda, E., Reyes C., (2002), "Approximate lateral drift demands in multistory buildings with nonuniform stiffness", Journal of Structural Engineering, July 2002, 840-849.

Miranda, E., Taghavi, S., (2005), "Approximate Floor Acceleration Demands in Multi-Story Buildings. I. Formulation", Journal of Structural Engineering, February 2005, 203-211.

Miranda, E., Taghavi, S., (2005), "Approximate Floor Acceleration Demands in Multi-Story Buildings. II. Applications", Journal of Structural Engineering, February 2005, 212-220.

De la Llera, J.C., and Chopra, A.K., (1998), "Evaluation of seismic code provisions using strong-motion building records from the 1994 Northridge earthquake", UCB/EERC-97/16, Earthquake Engineering Research Center, University of California, Berkeley.

Acknowledgements

Research supported by the U.S. Geological Survey (USGS), Department of the Interior, under USGS awards No. 07HQGR0073 and 07HQGR0065. The views and conclusions contained in this document are those of the authors and should not be interpreted as necessarily representing the official policies, either expressed or implied, of the U.S. Government.

Bibliography

He Liu, Mansheng Wang, Yibin Zheng and Xiyuan Zhou, “Identification of the inter-story stiffness of shear type structures using the extended Kalman filer”, Proceeding of the “World Forum on Smart Materials and Smart Structures Technology” Chongqing & Nanjing, China, May 22-27, 2007.